

RESEARCH

Open Access



Continuous collection of human mesenchymal-stromal-cell-derived extracellular vesicles from a stirred tank reactor operated under xenogeneic-free conditions for therapeutic applications

Cristiana Ulpiano^{1,2}, William Salvador^{1,2†}, Teresa Franchi-Mendes^{1,2†}, Min-Chang Huang³, Yee-Hsien Lin³, Han-Tse Lin³, Carlos A. V. Rodrigues^{1,2}, Ana Fernandes-Platzgummer^{1,2}, Joaquim M. S. Cabral^{1,2}, Gabriel A. Monteiro^{1,2} and Cláudia L. da Silva^{1,2*} 

Abstract

Background Mesenchymal-stromal-cell-derived extracellular vesicles (MSC-EVs) play a key role in the paracrine effects of MSC and have demonstrated therapeutic potential in various preclinical models. However, clinical translation is hindered by manufacturing practices relying on planar culture systems, fetal bovine serum (FBS)-supplemented media, and non-scalable, low-purity EV isolation methods that fail to meet dose and safety requirements, underscoring the need for innovative approaches. In this study, we developed a scalable platform to manufacture human MSC-EVs at clinically relevant numbers, integrating continuous collection of EV-enriched conditioned media (CM) using a stirred-tank reactor (STR) under xenogeneic-free conditions and a scalable downstream process.

Methods Wharton's jelly-derived MSC (MSC(WJ)) were expanded using microcarriers in a controlled STR using human platelet lysate (hPL)-supplemented medium. Then, a 3-day EV production stage, featuring continuous harvesting of the CM, was established using a novel serum-/xeno(geneic)-free exosome depleted-hPL supplement. For the isolation of MSC-EVs, a scalable process was implemented by pairing tangential flow filtration and anion exchange chromatography. Isolated MSC-EVs were characterised using nanoparticle tracking analysis, protein and

[†]William Salvador and Teresa Franchi-Mendes contributed equally to this work.

Gabriel A. Monteiro and Cláudia Lobato da Silva share senior authorship.

*Correspondence:
Cláudia L. da Silva
claudia_lobato@tecnico.ulisboa.pt

Full list of author information is available at the end of the article



© The Author(s) 2025. **Open Access** This article is licensed under a Creative Commons Attribution-NonCommercial-NoDerivatives 4.0 International License, which permits any non-commercial use, sharing, distribution and reproduction in any medium or format, as long as you give appropriate credit to the original author(s) and the source, provide a link to the Creative Commons licence, and indicate if you modified the licensed material. You do not have permission under this licence to share adapted material derived from this article or parts of it. The images or other third party material in this article are included in the article's Creative Commons licence, unless indicated otherwise in a credit line to the material. If material is not included in the article's Creative Commons licence and your intended use is not permitted by statutory regulation or exceeds the permitted use, you will need to obtain permission directly from the copyright holder. To view a copy of this licence, visit <http://creativecommons.org/licenses/by-nc-nd/4.0/>.

zeta potential quantification, western blot analysis of EV protein markers, transmission electron microscopy and uptake studies of fluorescently labelled-EVs.

Results The system sustained the efficient expansion of MSC(WJ), reaching a total of $(6.03 \pm 0.181) \times 10^7$ cells after 7 days, which corresponds to a 30.1 ± 0.740 -fold expansion. Upon a 3-day continuous CM harvesting, a total of $(2.13 \pm 0.301) \times 10^{12}$ EVs were isolated corresponding to a particle yield factor of $(1.26 \pm 0.186) \times 10^4$ EVs/cell/day. MSC-EVs presented high purity levels $(5.53 \pm 1.55) \times 10^9$ particles/ μ g, a homogeneous small size distribution (mean diameter of 115 ± 4.88 nm), a surface charge of -23.4 ± 6.23 mV, positive detection of tetraspanins CD9 and CD63 and syntenin-1 and displayed a typical cup-shaped morphology. MSC-EVs were readily incorporated by endothelial cells and two human breast cancer cell lines.

Conclusions Overall, the scalable and Good Manufacturing Practices (GMP)-compliant platform established herein enabled the reproducible manufacturing of MSC-EVs with high purity and generally accepted characteristics concerning size, protein markers, surface charge, morphology, and cellular internalization, validating its potential for future clinical applications.

Keywords Extracellular vesicles, Mesenchymal stromal cells, Stirred-tank reactor, Continuous collection, Scalable manufacturing

Introduction

Extracellular vesicles (EVs) are small membrane-enclosed structures of 50–1,000 nm in diameter that are actively secreted by cells and harbour a variety of biologically active molecules, including proteins and nucleic acids [1]. Although originally identified as cellular waste, EVs are currently established as essential mediators of cell-cell communication that can induce alterations in nearby or distant recipient cells [1, 2]. EVs have the innate capacity to efficiently cross biological barriers and demonstrate reduced immunogenicity/toxicity, therefore being extensively investigated as potential intrinsic therapeutic agents, as well as drug delivery vehicles [3–5].

Mesenchymal stromal cells (MSC) are among the most extensively studied EV-producing cell types [6]. MSC-derived EVs (MSC-EVs) are an important component of the paracrine action of MSC in tissue repair and regeneration [7]. Like their parental cells, MSC-EVs demonstrate immunomodulatory and anti-apoptosis properties and the ability to regulate endogenous cell functions [8, 9]. While MSC have been thoroughly evaluated in clinical trials for various conditions and have demonstrated an exceptional safety profile [10–12], MSC-EVs can potentially offer additional safety advantages as they do not self-replicate and have a lower risk of microvasculature entrapment upon administration [13, 14]. Furthermore, MSC-EVs can be easily handled and endure different types of preservation [15]. These attributes position MSC-EVs as promising candidates for off-the-shelf, cell-free therapeutics. MSC-EVs have shown significant beneficial effects in various preclinical disease models, including ischemic stroke, chronic kidney injury and chronic obstructive pulmonary disease [8, 9, 16]. Moreover, MSC-EVs can be bioengineered to enhance their therapeutic cargo and improve their selectivity for target cells, making them promising drug delivery systems [17].

In clinical settings, large doses of MSC-EVs are required, ranging from 10^{10} to 10^{11} total administered vesicles [18]. For instance, an ongoing trial for treating acute respiratory distress syndrome (NCT04602104) involves daily aerosol inhalation of 1.6×10^9 MSC-EVs for a week. In another trial for osteoarthritis (NCT05060107), 5×10^{11} MSC-EVs are administered as a single intra-articular injection. However, conventional EV manufacturing methods employing planar culture systems (e.g. T-flasks) and ultracentrifugation (UC) lack scalability and generate low EV yields with limited purity, making them inadequate for clinical translation [19]. Thus, the implementation of innovative MSC-EV manufacturing workflows that include scalable and Good Manufacturing Practices (GMP)-compliant upstream and downstream processes is essential to generate high-purity EVs in clinically relevant numbers [19].

For large-scale MSC culture, bioreactor platforms combined with microcarriers offer a promising strategy to increase cell density and sustain the production of large volumes of EV-enriched conditioned media (CM) [19]. Moreover, shear stress associated with dynamic stirred culture conditions promotes higher EV secretion from MSC when compared to static conditions [20–24]. Multiple small-scale microcarrier-based stirred platforms, such as spinner flasks [23, 25, 26] and vertical-wheel systems [20, 21, 27], have been implemented to maximize MSC expansion and MSC-EV production. Stirred-tank reactors (STR), featuring higher reproducibility due to automated control, can further enhance EV yields and process standardization by continuously monitoring and controlling the cell culture environment [22, 24, 28].

Aside from the culture platform, another important factor in upscaling MSC-EV production is the MSC tissue source, as cell doubling rates and EV secretion vary significantly, affecting final product costs [19, 21]. Our

previous work consistently demonstrated higher EV concentration and productivity when using Wharton's jelly (WJ)-derived MSC (MSC(WJ)) compared to MSC isolated from adipose tissue (MSC(AT)) and bone marrow (MSC(M)), whether expanded in static conditions (i.e. T-flasks) or in vertical wheel bioreactors [21]. Similarly, others have reported that MSC(WJ) exhibit higher expansion rates and produce greater EV yields than MSC(M) and MSC(AT) [29], making MSC(WJ) particularly attractive for EV manufacturing. Selecting a suitable culture medium formulation is equally important, with serum-/xeno(geneic)-free (S/XF) options being indispensable for transitioning to GMP-compliant conditions, although most preclinical studies still use fetal bovine serum (FBS)-containing media formulations [30]. Moreover, during conditioning periods for EV collection, it is essential to use media depleted of EVs to avoid cross-contamination, while ensuring cell health and EV productivity to maintain process efficiency [30, 31]. For EV production, MSC are typically cultured in an EV-free medium after expansion during conditioning periods ranging from 24 to 72 h [21, 22, 32]. Our group has previously established platforms for MSC-EV production in stirred systems exploring various MSC sources, S/XF culture media, and conditioning periods [21, 26, 28].

Following upstream processing, a scalable downstream process that includes the concentration and separation of EVs from the contaminants present in the CM is required to manufacture MSC-EVs at a clinical scale. While UC is commonly used, it has limitations such as incomplete contaminant separation, lengthy processing times, and poor scalability [19, 33, 34]. More efficient alternatives for EV isolation include filtration- and chromatography-based techniques. Tangential flow filtration (TFF) allows for the efficient and reproducible processing of large volumes, yielding high EV quantities, and can be combined with chromatographic methods for enhanced purity [30, 35]. Anion exchange chromatography (AEC), for instance, exploits the interactions between negatively charged EVs and an anion exchanger with positively charged functional groups or cations [35]. This technique has already been used to isolate EVs from cell cultures, demonstrating increased EV recoveries compared to other methods, such as UC and ultrafiltration coupled with size-exclusion chromatography (SEC) [36, 37].

In this study, we implemented a scalable microcarrier-based STR platform to continuously harvest EVs and consequently enhance MSC-EV production yields. Human MSC(WJ) were used for the robust production of EVs, combining a STR with an S/XF EV-depleted human platelet lysate (hPL) supplemented medium. After efficient MSC expansion, this system allowed a continuous 3-day EV collection stage under stirred conditions without compromising cell viability. By integrating a fully

scalable downstream system composed of TFF followed by AEC, we established an MSC-EV manufacturing process that can comply with GMP standards and meet the clinical dose requirements. Our platform allowed reproducible, high-yield manufacturing of MSC-EVs with consistent and generally accepted characteristics concerning size, surface charge, purity, morphology and cellular internalization.

Materials and methods

MSC(WJ) isolation and expansion under static conditions

MSC were isolated from the Wharton's Jelly (MSC(WJ)) of human umbilical cord samples in hPL-supplemented medium according to the protocol described by Soure et al. [38]. Samples were obtained from healthy donors after written informed consent according to Directive 2004/23/EC of the European Parliament and of the Council of 31 March 2004 on setting standards of quality and safety for the donation, procurement, testing, processing, preservation, storage and distribution of human tissues and cells (Portuguese Law 22/2007, June 29), with the approval of the Ethics Committee of the respective clinical institution (Protocol iBB/SGO-CHLO n°. 1277, May 2012). Cryopreserved MSC(WJ) were thawed and plated on T-flasks at a cell density of 3,000 cells/cm² and cultured in low glucose Dulbecco's Modified Eagle's Medium (DMEM) (Gibco, Life Technologies), supplemented with 5% (v/v) of hPL UltraGRO™-PURE gamma-irradiated (GI) (AventaCell BioMedical) and 1% (v/v) Antibiotic-Antimycotic (A/A) (Gibco, Life Technologies) (DMEM-hPL). Cells were maintained at 37°C and 5% CO₂ in a humidified atmosphere. At 80% confluency, MSC(WJ) were detached with TrypLE™ Select Enzyme, 1x (Gibco, Life Technologies) for 7 min at 37°C. Cell number and viability were estimated using the Trypan Blue Solution, 0.4% (Gibco, Life Technologies) exclusion method.

MSC-EV containing conditioned medium (CM) production under static conditions

MSC(WJ) were seeded onto 6-well plates at 3,000 cells/cm² and cultured for 4–5 days (>90% confluency) in DMEM-hPL. Afterwards, culture medium was removed, and cells were washed twice with 1x phosphate-buffered saline (PBS), before subsequently being cultured in DMEM supplemented with 5% (v/v) of Exosome depleted hPL UltraGRO™-PURE GI (AventaCell BioMedical) and 1% (v/v) A/A (DMEM-hPL-EVd) for CM production. CM was collected at 24 h, 48 h and 72 h timepoints in two different modes; (i) without any medium renewal throughout 3 days; and (ii) with medium renewal every 24 h. MSC-EV containing CM was centrifuged at 2,000xg for 15 min, filtered using Millex-HV Syringe Filter Unit with Durapore® PVDF membrane, 0.45 µm (Millipore),

and stored at -80°C until total particle number quantification using Nanoparticle Tracking Analysis (NTA), as described below.

MSC(WJ) expansion and CM production in stirred-tank reactors

MSC(WJ) from three independent donors (passages 4–5) were cultured for 10 days in a 250 mL glass DASbox Mini Bioreactor System (Eppendorf) equipped with an 8-blade 60° -pitch impeller and sensors for monitoring temperature, pH and dissolved oxygen. The glass vessel was treated with the siliconizing reagent Sigmacote® (Sigma-Aldrich) before use. DASware® control software (Eppendorf™) was employed to control the process parameters within the chosen set points ($T=37^{\circ}\text{C}$ and $\text{pH}=7.2$). Oxygen was supplied to the stirred tank reactor (STR) by the introduction of 100% air, corresponding to 21%

pure O_2 , through the headspace. A schematic workflow of the culture parameters used in the MSC(WJ) expansion and MSC-EV production stages in a fully controlled STR system is depicted in Fig. 1. Essentially, two million cells were seeded onto $1,080\text{ cm}^2$ of Synthamax II-coated Dissolvable Microcarriers (Corning®), corresponding to a seeding density of approximately $1,850\text{ cells/cm}^2$, and inoculated into the STR with an initial working volume of 80 mL. During the 7-day cell expansion stage, MSC(WJ) were cultured in DMEM-hPL with an intermittent agitation regime of 5 min at 50 rpm and 30 min at 0 rpm [26]. From day 1 to day 4, continuous fed-batch was performed at a constant rate of 1.92 mL/h until reaching a volume of 160 mL. From day 5 to day 7, medium perfusion at a constant rate of 3.33 mL/h was carried out until completely replacing the medium. A micro sparger with a pore size of $10\text{ }\mu\text{m}$ was employed as a filter to ensure the retention

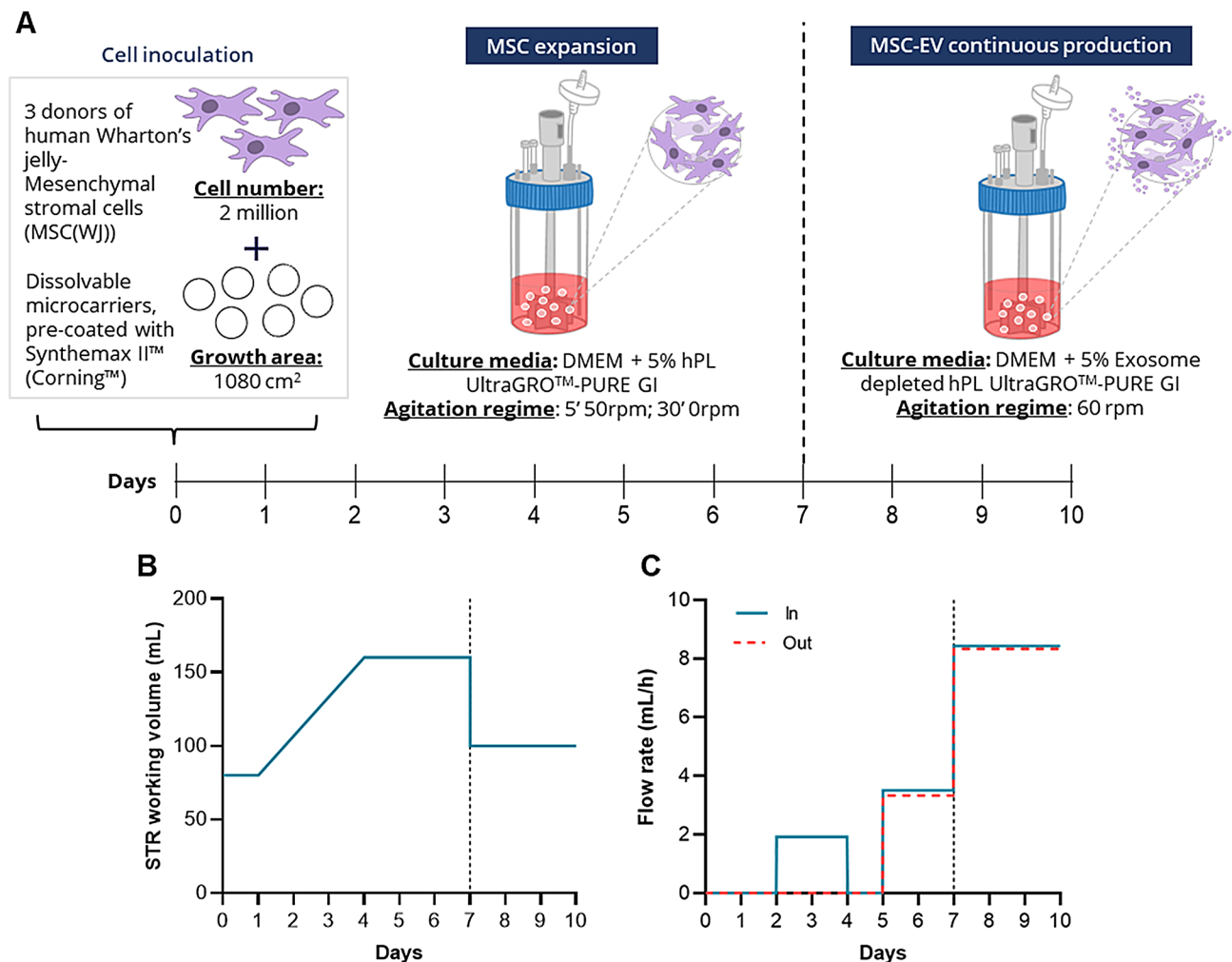


Fig. 1 Schematic of the culture parameters used for microcarrier-based MSC(WJ) expansion and continuous EV production in a STR. **(A)** Schematic representation of cell inoculation conditions, culture medium and agitation regimens implemented throughout the MSC(WJ) expansion and EV production stages. **(B)** STR working volume during MSC(WJ) expansion and EV production. **(C)** Culture medium flow rate in and out of the STR during MSC(WJ) expansion and EV production. Stages are separated by the dashed line. MSC(WJ), Wharton's jelly-derived mesenchymal stromal cells; EVs, extracellular vesicles; STR, stirred tank reactor

of microcarriers during perfusion. Before the subsequent MSC-EV production stage, cell-containing microcarriers were washed with 200 mL of PBS and resuspended in 100 mL DMEM-hPL-EVd. During the 3-day MSC-EV production stage, the agitation was set to 60 rpm and CM was collected through perfusion at a rate of 8.33 mL/h, which corresponds to a production of 200 mL of CM per day. Each day, MSC-EV-containing CM was precleared from cell debris by centrifugation at 2,000xg for 15 min, followed by filtration using a Stericup® Quick Release Durapore® PVDF membrane 0.45 µm (Millipore) bottle-top filter and stored at -80 °C until total particle number quantification using NTA and EV isolation, as described below.

Monitoring of culture parameters and cell imaging on microcarriers

Cell number quantification

Throughout the 10-day STR cultures, cell number assessment was performed as described in Bandarra-Tavares et al. [26] by collecting two independent 1 mL samples of MSC(WJ) culture from the STR at 60 rpm. For cell detachment, microcarriers were washed twice with PBS and enzymatically digested, for 7 min at 37 °C and 600 rpm in Thermomixer® comfort (Eppendorf AG), with 0.5 mL of a solution composed of 2.6% Pectinase (Sigma-Aldrich), 2% EDTA (Sigma-Aldrich) and 95.4% TrypLE™ 1x. The reaction was stopped by adding 1 mL of DMEM-hPL and the total number of viable cells was estimated using the Trypan Blue exclusion method. The specific growth rate (μ_{max}) and doubling time (td) of MSC(WJ) during the exponential growth phase were calculated as described in Fernandes-Platzgummer et al. [28].

Glucose and lactate concentrations analysis

For glucose and lactate monitoring, the supernatant of daily samples retrieved from the STR was centrifuged at 360xg for 10 min. Glucose and lactate concentrations were determined through membrane-bound immobilized enzyme quantification using the YSI 2500 Biochemistry Analyser (Yellow Springs Instrument).

Cell viability and distribution on the microcarriers

Additional 0.5 mL samples of MSC(WJ) culture from the STR were collected for cell imaging on microcarriers. Cell distribution on the microcarriers was evaluated by nuclei staining with 4',6-diamidino-2-phenylindole (DAPI) (Sigma-Aldrich) at 1 µg/mL. Cell viability on microcarriers was assessed by staining viable cells with Calcein-AM (Sigma-Aldrich) at 1 µM. Additionally, on day 10 of STR culture, dead cells were stained using Ethidium Homodimer III at 1 µM. Images were acquired using a fluorescence microscope DMI 3000B (Leica).

MSC(WJ) harvesting and characterization after STR culture

At the end of the STR culture (day 10), MSC(WJ) were harvested from the microcarriers inside the STR vessel. After CM removal through the perfusion filter, cell-containing microcarriers were washed with 200 mL of PBS and subsequently digested with 55 mL of microcarrier dissolution solution at 37°C and 100 rpm for 15–20 min, resulting in cell detachment. The reaction was stopped by adding 55 mL of DMEM-hPL and MSC(WJ) were centrifuged and collected for further characterization according to the criteria defined by the International Society for Cell and Gene Therapy (ISCT) [39]. Immunophenotypic analysis of MSC(WJ) was performed by flow cytometry with a panel of anti-human monoclonal antibodies: CD90-PE, CD44-PerCP-Cy5.5, CD73-FITC, CD105-PE, CD34-FITC, HLA-DR-FITC, CD80-PE, CD45-PerCP-Cy5.5, CD19-FITC (Becton Dickinson, BD). LIVE/DEAD™ Fixable Far Red Dead Cell Stain Kit (Invitrogen, Life Technologies) was used to assess cell viability. Samples were acquired with a minimum of 10,000 events using a BD FACSCalibur™ Flow Cytometer (BD) and data was analysed using FlowJo™ Software (BD).

MSC(WJ) multilineage differentiation capacity was also evaluated. For osteogenic and adipogenic differentiation, MSC(WJ) were seeded onto 24-well plates at 3,000 cells/cm² and cultured for 4–5 days in DMEM-hPL. Afterwards, the culture medium was replaced by the respective differentiation medium, StemPro™ Adipogenesis Differentiation Kit or StemPro™ Osteogenesis Differentiation Kit (Gibco). For chondrogenic differentiation, spheroids composed of 100,000 cells were generated by applying the hanging-drop technique. After 24 h, the spheroids were placed onto ultra-low attachment 24-well plates (Corning) with Mesencult™-ACF Chondrogenic Differentiation Kit (STEMCELL Technologies) medium. Differentiation medium was replaced twice a week for 21 days. Following this, adipocyte-produced lipid droplets were stained with Oil Red O, osteocyte progenitors were stained with alkaline phosphatase and chondrocyte-secreted extracellular matrix proteins were stained as described in Santos et al. [40].

Isolation of MSC-EVs from conditioned media

The CM collected from the reactor (i.e. 3 day-conditioning phase) was thawed on ice and pooled for MSC-EV isolation. A schematic representation of the EV isolation process is represented in Supplementary Fig. 1. The employed EV purification method was adapted from Silva et al. [36]. Firstly, by using a Minimate™ EVO Tangential flow filtration (TFF) system, the 600 mL of CM was concentrated/diafiltrated using a Minimate™ 100 kDa MWCO Omega™ Membrane (Cytiva) to a volume of 50 mL of nuclease buffer composed of 50 mM Tris-HCl (Thermo Scientific™), 20 mM NaCl (Thermo Scientific™),

pH 8. The diafiltrated sample was then supplemented with 5 mM of CaCl_2 and digested with 5U (per mL of initial CM) of Micrococcal nuclease (MNase, Thermo Scientific™) for 75 min at 37°C with 600 rpm agitation in the Thermomixer® comfort (Eppendorf AG). Afterwards, the digested sample was concentrated/diafiltrated to a volume of 20 mL of chromatography buffer A (50 mM HEPES, 20 mM NaCl, pH 7). Subsequently, anion exchange chromatography (AEC) was performed using a Tricorn 5/50 column (Cytiva) packed with 1 mL of Capto™ Q ImpRes resin (Cytiva) connected to an ÄKTA Purifier 10 system (Cytiva). The column was pre-equilibrated with a buffer composed of 50 mM HEPES, 180.7 mM NaCl, pH 7, (10.5% buffer B (50 mM HEPES, 2 M NaCl, pH 7), ≈ 23 mS/cm). The EV-containing sample was pre-conditioned with 10.5% buffer B and three chromatographic runs using a 10 mL volume sample were performed. Unbound material was washed with 15 column volumes (CV) of 10.5% B, and stepwise elution was completed with 10 CV of 60% B (≈ 95 mS/cm) and 7 CV of 100% B (≈ 142 mS/cm). Finally, the EV-containing fractions were concentrated/diafiltrated to a volume of approximately 0.5 mL in PBS using an ultrafilter with a molecular weight cut-off of 30 kDa (Amicon® Ultra-4, Merck Millipore) previously passivated overnight with a solution 5% (v/v) Tween-20 in distilled water.

Characterization of isolated MSC-EVs

Nanoparticle tracking analysis (NTA)

Particle quantification and size distribution profiles of EV-containing CM and isolated MSC-EV samples were obtained by Nanoparticle tracking analysis (NTA) using a Nanosight LM14C instrument (Malvern). Samples were diluted in PBS to achieve a final particle concentration ranging between 10^8 and 10^9 particles/mL and measured using the standard operation procedure (SOP) as follows: camera level 13; screen gain 1; time of acquisition 30 s; number of captures 5 (each capture with fresh sample). Video recording was acquired and analysed using NanoSight NTA version 3.4 (Malvern).

Protein quantification

Total protein of isolated MSC-EVs samples was determined using Micro BCA™ Protein Assay Kit (Thermo Scientific™) according to manufacturer's instructions for the microplate procedure. Samples were lysed in RIPA buffer (Merck Millipore) 1x at room temperature for 10 min and diluted 10 times in PBS. Sample concentration was determined by applying a second-order polynomial curve fit to the bovine serum albumin (BSA) standards prepared in 0.1x RIPA in PBS solution. Absorbance was measured at 562 nm using the plate reader (Infinite® 200 PRO, NanoQuant, Tecan Trading AG). Two replicates were quantified for each sample. To assess the purity of the MSC-EV

samples, the particle-to-protein ratio (PPR), which consists of the ratio between the total particle number and total protein of the sample [33], was determined.

Zeta potential

MSC-EV samples were diluted 10,000 times in distilled water. Samples were loaded into disposable capillary cells DTS1070 (Malvern Instruments) and analysed using the SOP set up for a sample refractive index of 1.45 (protein), dispersant refractive index of 1.33 (water), system temperature of 25 °C, and sample equilibration time of 2 min. Each sample was measured in 3 runs, each resulting from subruns ranging from 10 to 100 in automatic mode. Measurements were performed with a Zetasizer Nano ZS (Malvern), and Malvern Zetasizer software version 7.10 was used to collect and analyse the data.

Western blot analysis of EV protein markers

The positive EV-protein markers CD9, CD63, Syntenin-1 and the negative marker Calnexin were evaluated in isolated MSC-EV samples using Western blot, with whole cell lysate (WCL) of MSC(WJ) harvested from the STR cultures used as control. For the WCL samples, cells were lysed in RIPA buffer 1x supplemented with cComplete™ Protease Inhibitor Cocktail (Roche) and centrifuged at 12,000xg for 15 min at 4 °C, after which supernatants were recovered. EV and WCL samples (2 µg of total protein, corresponding to $\sim 1 \times 10^{10}$ EVs) were diluted in PBS, NuPAGE™ LDS Sample buffer and NuPAGE™ Sample Reducing Agent (Invitrogen, Life Technologies) (except for tetraspanin detection, where non-reducing conditions were used), denatured at 95 °C for 10 min and loaded in 4–12% Bis-Tris polyacrylamide precast gels (Invitrogen, Life Technologies). Electrophoresis was run at 130 V in MES SDS Running Buffer for 1 h and the proteins were subsequently transferred into nitrocellulose membranes using a Power Blotter System (Invitrogen, Life Technologies). Membranes were blocked with 5% BSA solution in 1x Tris Buffered Saline with Tween (TBST) for 1 h at room temperature and incubated overnight at 4 °C with primary antibodies anti-CD9 (CBL162, Merck), anti-CD63 (556019, BD), anti-Calnexin (610523, BD) and anti-Syntenin-1 (ab133267, Abcam) at 1:1000 concentration. After extensive washing with TBST, membranes were incubated with HRP-conjugated secondary antibodies anti-Mouse (G-21040, Invitrogen) and anti-Rabbit (HAF008, R&D Systems) at 1:20,000 concentration for 1 h at RT. Finally, after secondary antibody washing with TBST, SuperSignal™ West Pico PLUS Chemiluminescent Substrate (Thermo Scientific™) was applied for membrane revelation according to manufacturer's instructions. Images were acquired using an iBright™ CL1500 Imaging System (Invitrogen, Life Technologies).

Transmission electron microscopy (TEM)

Transmission electron microscopy (TEM) imaging of negatively stained MSC-EV samples was conducted as described in Fernandes-Platzgummer et al. [28], using a Tecnai G2 Spirit BioTWIN Transmission Electron Microscope (FEI Company™) with an Olympus-SIS Veleta CCD Camera.

EV uptake by target cells

Human umbilical vein endothelial cells (HUVECs), and human breast cancer cell lines MDA-MB-231 and MCF-7 were used as target cells for the EV uptake assays. HUVECs were obtained from Lonza and cultured in EGM-2 Endothelial Cell Growth Medium-2 (Lonza). MDA-MB-231 (HTB-26™) and MCF-7 (HTB-22™) cell lines were obtained from American Type Culture Collection (ATCC) and cultured in high-glucose DMEM (Gibco) supplemented with 10% (v/v) FBS (Gibco) and 1% (v/v) A/A.

Isolated MSC-EVs were labelled with the fluorescent dye AlexaFluor 647 NHS ester (Invitrogen, Thermo Scientific™). EVs ($3\text{--}4 \times 10^{10}$ EVs) were mixed with sodium bicarbonate (pH 8.3, 100 mM final concentration) and 0.625% v/v AlexaFluor 647 NHS ester (10 mg/mL in DMSO) and incubated for 1 h at 37 °C and 450 rpm. EVs were then diluted in PBS and quenched in 100 mM Tris-HCl in a final volume of 100 μ L, for 20 min at RT. Mock dye treatments were prepared by replacing the EVs with PBS. Labelled-EVs were immediately purified from unbound dye using Exosome Spin Columns MW3000 (Invitrogen) according to manufacturer instructions.

The day before the EV uptake experiment, HUVEC, MDA-MB-231 and MCF-7 (50,000 cells) were plated onto flat-bottom 96-well plates. Labelled-EVs were then added to the target cells at a concentration of approximately 2×10^{10} particles/mL in culture medium supplemented with Exosome-depleted FBS (Gibco) and incubated for 6 h at 37 °C. Afterwards, cells were harvested and analysed by flow cytometry using the FACSCalibur™ or FACSCanto™ Flow Cytometer (BD). The percentage of EV-containing cells and the relative EV uptake based on median fluorescence intensity (MFI) values (ratio of labelled-EV MFI to mock dye MFI) were analysed using the FlowJo™ Software (BD).

Statistical analysis

Statistical analysis was carried out using GraphPad Prism 9 software. Data were collected from three independent experiments and depicted as mean \pm standard error of the mean (SEM). Statistical tests are detailed in each figure legend, and all significant differences are indicated in the graphs.

Results

Medium renewal enhances particle production by MSC(WJ) under static conditions

To evaluate cell fitness and particle accumulation in the CM throughout 72 h, MSC(WJ) were cultured for 24 h, 48 h and 72 h periods under static conditions with/without medium renewal, every 24 h, using EV-depleted hPL (hPL-EVd) as culture medium supplement (Fig. 1). After 72 h, MSC(WJ) cultured in DMEM-hPL-EVd showed high cell survival with viability of $99.3 \pm 0.543\%$ and $98.9 \pm 0.158\%$, with and without 24 h-medium renewal, respectively, and presented typical cellular morphology (Fig. 2A). Additionally, no significant alterations in cell number were observed throughout the 72 h and the number of MSC(WJ) cultured with/without medium renewal every 24 h was comparable (Fig. 2B). The total number of particles in CM was similar across different conditioning periods with no medium replacement, indicating that there was no accumulation of particles over time (Fig. 2C). Moreover, the total number of particles secreted by MSC(WJ) was superior when cells were cultured with 24 h-medium renewal cycles compared to cells cultured without medium renewal ($9.78 \pm 2.34 \times 10^{10}$ vs. $6.26 \pm 0.382 \times 10^{10}$ at 48 h and $1.48 \pm 0.249 \times 10^{11}$ vs. $5.14 \pm 0.538 \times 10^{10}$ at 72 h) (Fig. 2C). After 72 h, 24 h-medium renewal allowed a significant fold increase of 2.84 ± 0.172 in the total number of particles produced by MSC(WJ), compared to when no medium was exchanged (Fig. 2C). This demonstrates that several EV collection cycles using the same parental cells can be performed, potentially maximising EV production.

MSC(WJ) expansion and continuous EV collection were accomplished in a microcarrier-based STR culture system

Based on the previous work performed by our group [21, 26, 28], a S/XF microcarrier-based STR culture system was implemented envisioning the continuous production of MSC-EVs. This system combines the use of Dissolvable microcarriers and hPL-supplemented medium for the expansion of MSC(WJ) followed by continuous production of EVs aided by a novel EV-free hPL supplement particularly developed for EV manufacturing (Fig. 1A). Initial adhesion efficiency of MSC(WJ) to microcarriers was $86.4 \pm 4.14\%$ on day 1 of STR culture and the cells were successfully expanded, with a maximum fold-expansion of 30.1 ± 0.740 achieved after 7 days. As seen in the growth curves represented in Fig. 3A, the cells exhibited exponential growth until reaching $(6.03 \pm 0.181) \times 10^7$ cells on day 7, corresponding to a cell density of $(3.77 \pm 0.113) \times 10^5$ cells/mL and $(5.58 \pm 0.168) \times 10^4$ cells/cm². The calculated growth rate (μ_{\max}) and duplication time (t_d) were $0.552 \pm 0.0274 \text{ day}^{-1}$ and 1.27 ± 0.0667 days, respectively. During the EV production stage between days 7 and 10, using DMEM-hPL-EVd, no significant

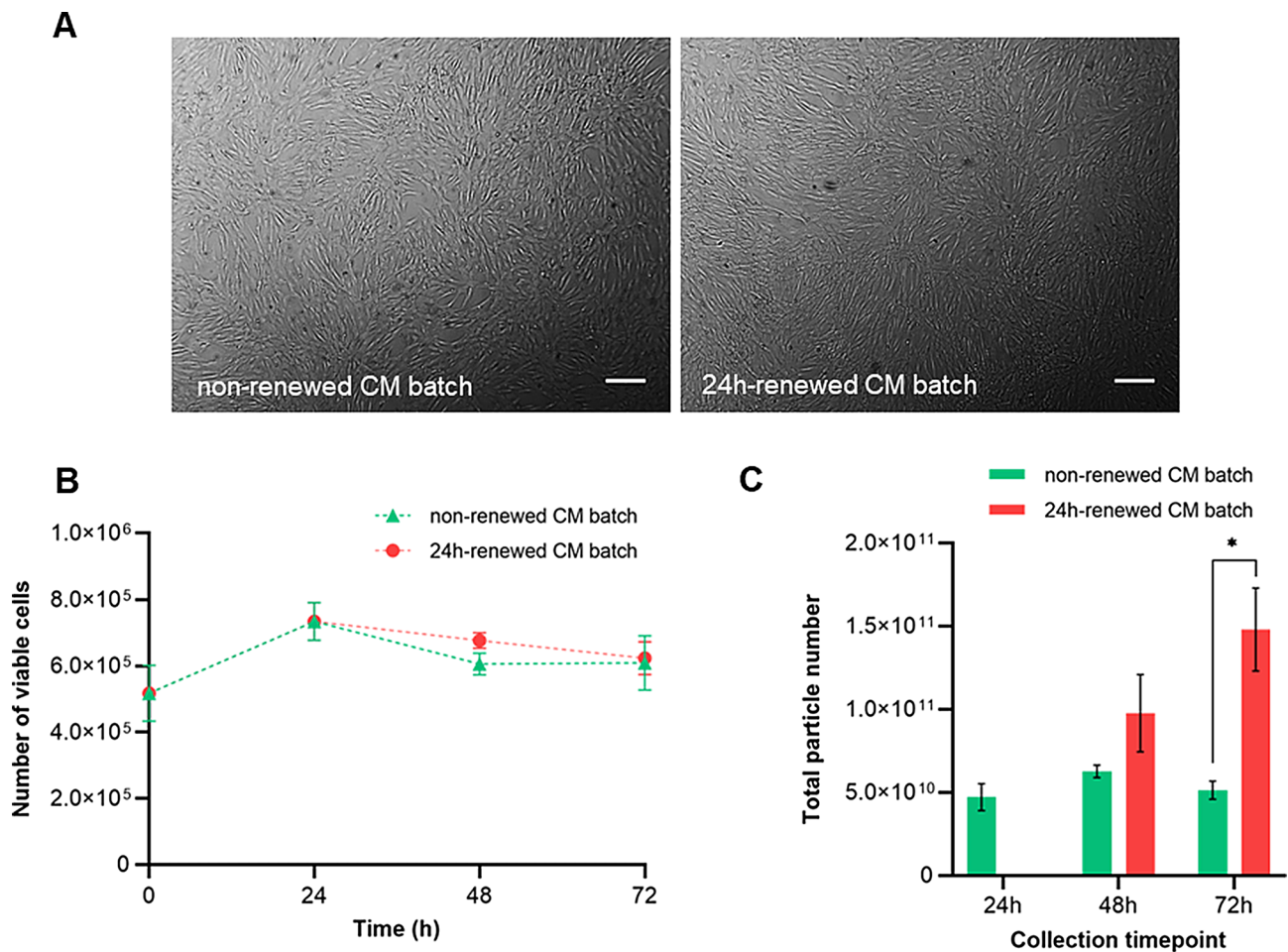


Fig. 2 Evaluation of particle accumulation in CM of MSC(WJ) cultured for 72 h under static conditions. **(A)** Representative images of MSC(WJ) morphology at the end of the 72 h-conditioning period, with (right) or without (left) medium renewal every 24 h. Scale bar: 250 μ m. **(B)** Total number of viable cells cultured without any medium renewal (green) and with medium renewal every 24 h (red). **(C)** Total number of particles produced up to the respective timepoint, without any medium renewal (green) and with medium renewal every 24 h (red), determined from NTA measurements. Graph values are presented as mean \pm SEM of 3 independent donors ($n=3$). Statistical analysis was performed using a one-way ANOVA followed by a post-hoc Tukey's multiple comparisons test; $*p < 0.05$. CM, conditioned medium; MSC(WJ), Wharton's jelly-derived mesenchymal stromal cells; NTA, nanoparticle tracking analysis

alteration in cell number was observed and cell concentration remained relatively constant at $(5.58 \pm 0.277) \times 10^5$ cells/mL.

The level of occupancy of the microcarriers throughout MSC(WJ) expansion was evaluated by nuclei staining, through which a progressive increase in the number of cell-loaded microcarriers was observed from days 1 to 7, along with a gradual increase in microcarrier occupancy (Fig. 3B). This increase was accompanied by microcarrier aggregation as MSC(WJ) expansion reached higher cell densities, being most evident from day 6 onwards (Fig. 3B, C). Calcein-AM staining showed viable cells presenting the characteristic elongated morphology of MSC on microcarrier surfaces throughout STR culture, including during the EV production stage (Fig. 3C). Moreover, Live/Dead images of MSC(WJ) on microcarriers on day 10 of STR culture showed a negligible number of dead

cells after cell expansion and EV production (Supplementary Fig. 2). Glucose and lactate concentration analysis demonstrated that the adopted feeding scheme (Fig. 1C) successfully prevented glucose depletion and lactate accumulation above critical concentration [41] throughout the 10-day culture (Fig. 3D). During the EV production stage, glucose and lactate concentrations were maintained constant around 4mM and 2mM, respectively (Fig. 3D). NTA measurements of the CM corresponding to each collection period during the 3-day EV production stage showed no significant differences in the number of total accumulated particles and the particle secretion rate by MSC(WJ), demonstrating an average particle yield factor before EV isolation of $(6.32 \pm 0.266) \times 10^4$ particles/cell/day (Fig. 3E). The collected CM had an average particle concentration of $(1.79 \pm 0.129) \times 10^{10}$ particles/mL. Overall, medium supplementation with hPL-EVd allowed

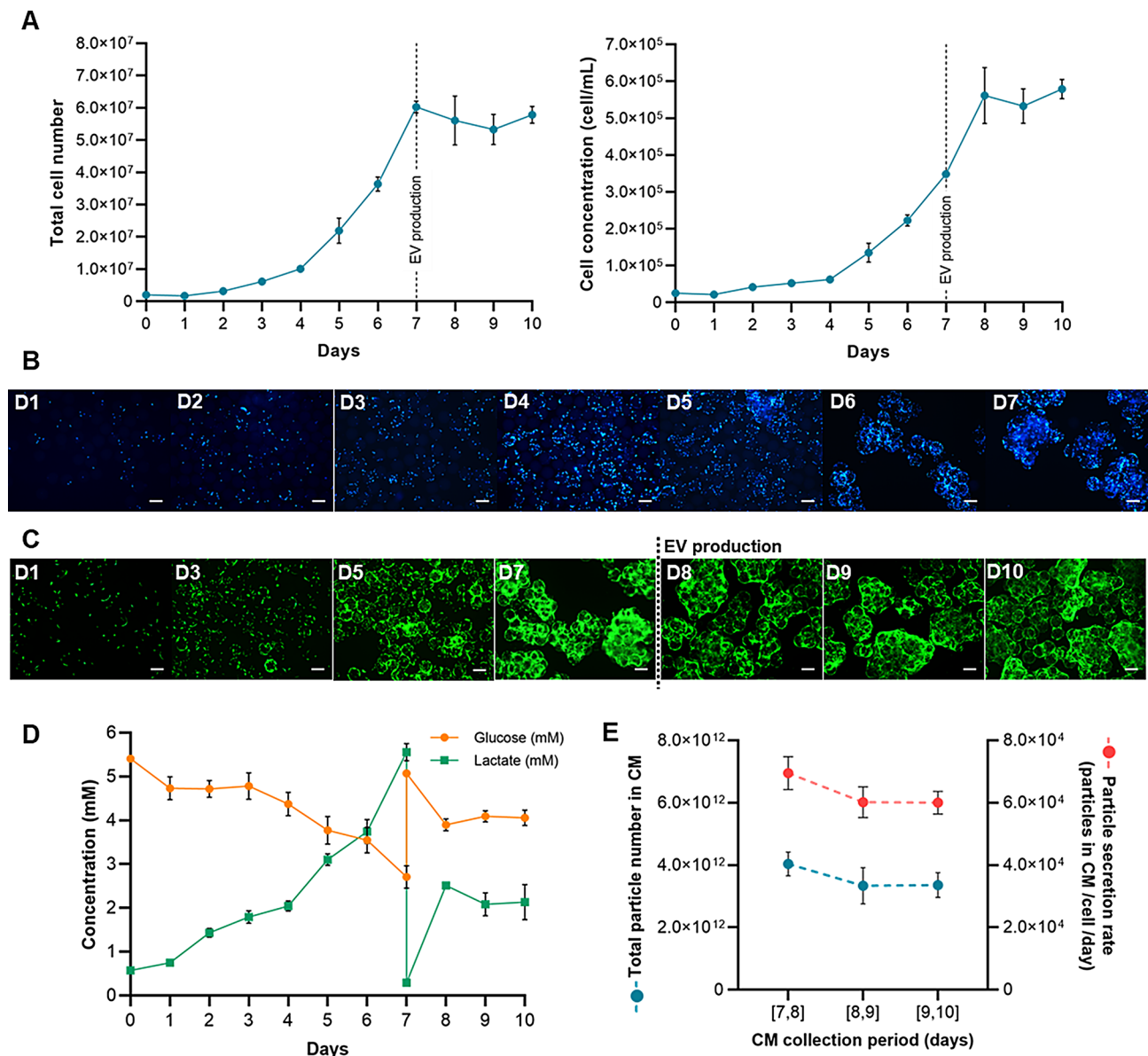


Fig. 3 Microcarrier-based expansion of MSC(WJ) and subsequent continuous EV production in a fully controlled STR system. **(A)** Growth curve of MSC(WJ) throughout the 10-day culture in STR depicted as total cell number (left) and cell concentration (right). The EV production stage started on day 7 and is highlighted by the dashed line. **(B)** Representative images of cell distribution on microcarriers throughout MSC(WJ) expansion in a STR, obtained through DAPI staining (blue). **(C)** Representative images of cell viability assessment throughout STR culture, obtained through Calcein-AM staining (green). MSC(WJ) expansion and EV production stages are separated by the dashed line. **(D)** Glucose and lactate concentration measurements throughout STR culture. **(E)** Total particle number (blue) and particle secretion rate of MSC(WJ) (red) throughout the 3-day EV production stage, determined from the NTA measurements of the CM of each day. Scale bar: 250 μ m. Graph values are presented as mean \pm SEM of 3 independent donors ($n=3$). No statistically significant differences were found using a one-way ANOVA followed by a post-hoc Tukey's multiple comparisons test. MSC(WJ), Wharton's jelly-derived mesenchymal stromal cells; EV, extracellular vesicle; STR, stirred tank reactor; DAPI, 4',6-diamidino-2-phenylindole; NTA, nanoparticle tracking analysis; CM, conditioned medium

the continuous production of EV-enriched CM under stirred conditions without causing significant alterations in the cell number, cell viability and particle secretion rate of MSC(WJ) (Fig. 3).

MSC(WJ) preserve their cellular identity upon EV collection in a STR

On day 10 of STR culture, following a 3-day continuous EV production, MSC(WJ) were harvested from the microcarriers using an enzymatic solution and characterized for viability, immunophenotype, and trilineage differentiation potential (Fig. 4) according to criteria

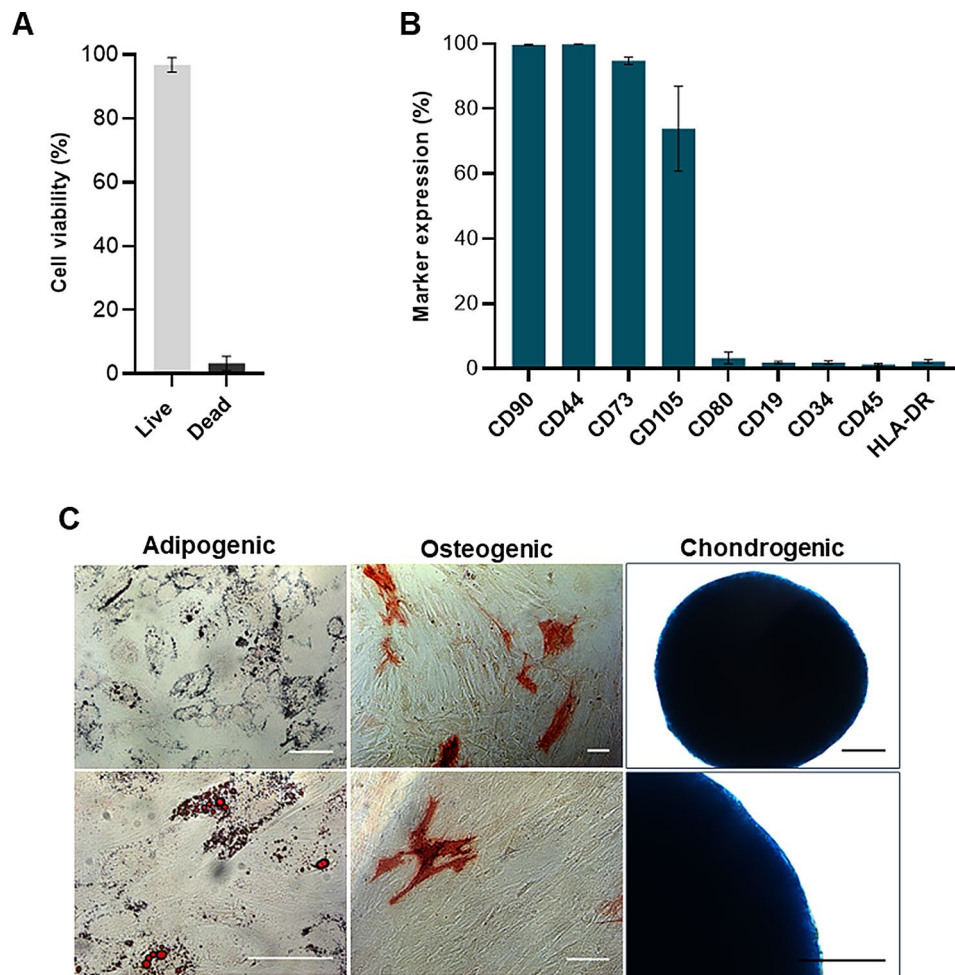


Fig. 4 Characterisation of MSC(WJ) after microcarrier-based cell expansion and continuous EV production in a STR system. **(A)** Cell viability after MSC(WJ) expansion and EV production in a STR, assessed by flow cytometry after Live/Dead staining. **(B)** Immunophenotypic analysis after MSC(WJ) expansion and EV production in a STR system through flow cytometry. **(C)** Trilineage differentiation potential of MSC(WJ) after expansion and EV production in a STR: Adipogenic lineage with adipocyte-produced lipid droplets stained using Oil Red O; Osteogenic lineage with osteocyte progenitors stained using Alkaline phosphatase; Chondrogenic lineage with staining of chondrocyte-secreted extracellular matrix proteins (Alcian Blue). Scale bar: 100 μ m. Graph values are presented as mean \pm SEM of 3 independent donors ($n=3$). MSC(WJ), Wharton's jelly-derived mesenchymal stromal cells; EV, extracellular vesicle; STR, stirred tank reactor

established by ISCT [39]. Harvested MSC(WJ) exhibited a high cell viability of $96.8 \pm 2.22\%$ (Fig. 4A), which was consistent with visual observations before the dissolution of microcarriers (Suppl Fig. 2), indicating that recovery from the beads had no significant adverse effect on cell viability. Immunophenotypic analysis demonstrated that, after EV production, MSC(WJ) expressed high levels ($\geq 95\%$) of positive cell surface markers CD90, CD44 and CD73 (Fig. 4B). The lower expression detected for positive marker CD105 ($74.9 \pm 13.1\%$) is not uncommon after cell expansion under stirred conditions [22, 28, 42, 43]. Moreover, the expression of negative markers CD80, CD19, CD34, CD45, and HLA-DR was negligible ($\leq 3\%$), further confirming MSC(WJ) immunophenotypic identity (Fig. 4B). After the conditioning stage, MSC(WJ) preserved their multilineage differentiation ability, further

validating their identity (Fig. 4C). MSC(WJ) successfully differentiated into: (i) the adipogenic lineage, confirmed by the detection of lipid droplets stained in red (left panel, Fig. 4C); (ii) the osteogenic lineage, validated by the presence of osteoblast progenitors stained in red (middle panel, Fig. 4C), and (iii) the chondrogenic lineage, corroborated by the blue staining of chondrocyte-secreted acidic polysaccharides (right panel, Fig. 4C).

Continuously harvested MSC(WJ)-EVs showed robust quality attributes after processing

After the 3-day continuous harvesting, EVs were successfully isolated from the CM of MSC(WJ) cultures using a scalable process (Supplementary Fig. 1). After CM filtration and concentration using TFF and nucleic acid digestion, AEC allowed further separation of soluble

proteins from EVs. The protein contaminants were eluted in the flowthrough, while the resin-adsorbed EVs were subsequently eluted by increasing the ionic strength (Supplementary Fig. 3). EV-containing fractions were concentrated and characterised following the criteria proposed by the International Society for Extracellular Vesicles (ISEV) [44]. A summary of the characteristics of the isolated MSC-EVs and yields is displayed in Table 1. NTA was used to determine the size distribution of isolated MSC-EVs, demonstrating an enrichment in particles below 200 nm (Fig. 5A) with a mean and mode diameter of approximately 115 ± 4.88 nm and 99.0 ± 8.97 nm, respectively (Table 1). Particle quantification confirmed the total isolation of $(2.13 \pm 0.301) \times 10^{12}$ EVs (Table 1) at a concentration of $(4.04 \pm 0.746) \times 10^{12}$ EVs/mL, which corresponds to a specific EV productivity of $(3.77 \pm 0.557) \times 10^4$ isolated EVs per producing cell (Table 1). A particle yield factor of $(1.26 \pm 0.186) \times 10^4$ particles/cell/day (Table 1) was calculated as a measure of EV yield, as suggested by Grangier and colleagues [45]. TEM images confirmed the presence of individual vesicles of different sizes that display the spherical and cup-shaped structure typical of EVs (Fig. 5B), which results from membrane dehydration during sample preparation [46]. The zeta potential measurements of isolated MSC-EVs indicated a net negative surface charge of -23.4 ± 6.23 mV (Table 1), as expected. To assess the purity of EV samples, protein quantification (425.3 ± 75.96 μ g) was performed to determine the particle-to-protein ratio (PPR). The average PPR value obtained for the isolated EV samples was $(5.53 \pm 1.55) \times 10^9$ particles/ μ g (Table 1). The isolated MSC-EVs expressed three EV-positive protein markers, namely tetraspanins CD9 and CD63 and syntenin-1, as detected through western-blot (Fig. 5C). Detection was stronger in EV samples compared to whole cell lysate (WCL) controls, confirming the EV-enrichment of isolated samples. Moreover, the negative marker calnexin was not detected in EV samples, in contrast to WCL controls (Fig. 5C). Besides morphological characterisation of

MSC-EVs, an uptake assay was performed to validate cell internalization of the isolated MSC-EVs into target cells. MSC-EVs were stained with Alexa647 and incubated with breast cancer cell lines MDA-MB-231 and MCF-7, and HUVECs. After 6 h, the percentage of EV-containing cells was high (>95%) for every target cell type (top panel, Fig. 5D). Although the difference did not reach statistical significance, the relative EV internalization appeared higher for HUVECs compared to the breast cancer cell lines (bottom panel, Fig. 5D), suggesting a potential increased affinity for MSC-EV uptake.

Discussion

MSC-EVs have shown great promise as natural therapeutics and drug delivery vehicles in a wide range of pre-clinical disease models [17, 47]. Despite their potential, most preclinical studies still rely on planar culture systems and FBS-supplemented culture medium formulations for MSC expansion, while using non-scalable low-purity grade methods for MSC-EV isolation. These practices hinder their translation into the clinic by failing to meet the necessary dose and safety requirements. In this context, the implementation of a large-scale manufacturing workflow for MSC-EVs, incorporating scalable upstream and downstream processes, is needed to provide high-purity EV yields [19, 30, 34]. Envisioning industrialisation, multiple large-scale systems have been investigated for EV production, among which are two-dimensional multilayer flasks [48] and different bioreactor configurations, such as hollow-fiber bioreactors [49] and STR combined with microcarriers [22, 28]. In particular, several groups have been exploring scalable microcarrier-based stirred platforms for MSC-EV production, including spinner flasks [23, 25, 26, 50] and vertical-wheel systems [20, 21, 27]. However, while numerous reports describe the successful large-scale expansion of MSC in microcarrier-based, fully controlled STR systems [42, 51–56], only a few have applied them to EV manufacturing [22, 24, 28]. Still, STR systems offer relevant advantages, including scalability potential, process automation, continuous perfusion-based operation, and reduced labor requirements. Nevertheless, MSC-EV production typically involves collecting the EV-enriched CM in a single batch for 24 to 72 h upon the cell expansion stage [20–22, 26–28]. Our work builds on these advantages and introduces a novel approach that focuses on maximizing MSC-EV production yields by implementing a scalable microcarrier-based STR culture system designed to continuously harvest EVs over a 3-day period, rather than relying on traditional single-batch collections. To increase cell viability and consequently extend the cell conditioning period, we employed a novel S/XF EV-depleted supplement, enabling MSC-EV manufacturing in a more physiologically relevant environment. Others have explored

Table 1 Characteristics and yields of EVs isolated from the CM of MSC(WJ) cultured in a STR

EV parameter	Average value for 3 MSC(WJ) donors
Total isolated EV number	$(2.13 \pm 0.301) \times 10^{12}$
Average size (nm)	115 ± 4.88
Mode of size (nm)	99.0 ± 8.97
Zeta potential (mV)	-23.4 ± 6.23
Particle-to-protein ratio (total particles/ μ g protein)	$(5.53 \pm 1.55) \times 10^9$
Specific EV productivity (EV/cell)	$(3.77 \pm 0.557) \times 10^4$
Particle yield factor (EV/cell/day)	$(1.26 \pm 0.186) \times 10^4$

Table values are presented as mean \pm SEM of 3 independent donors ($n=3$). EVs, extracellular vesicles; MSC(WJ), Wharton's jelly-derived mesenchymal stromal cells; STR, stirred tank reactor

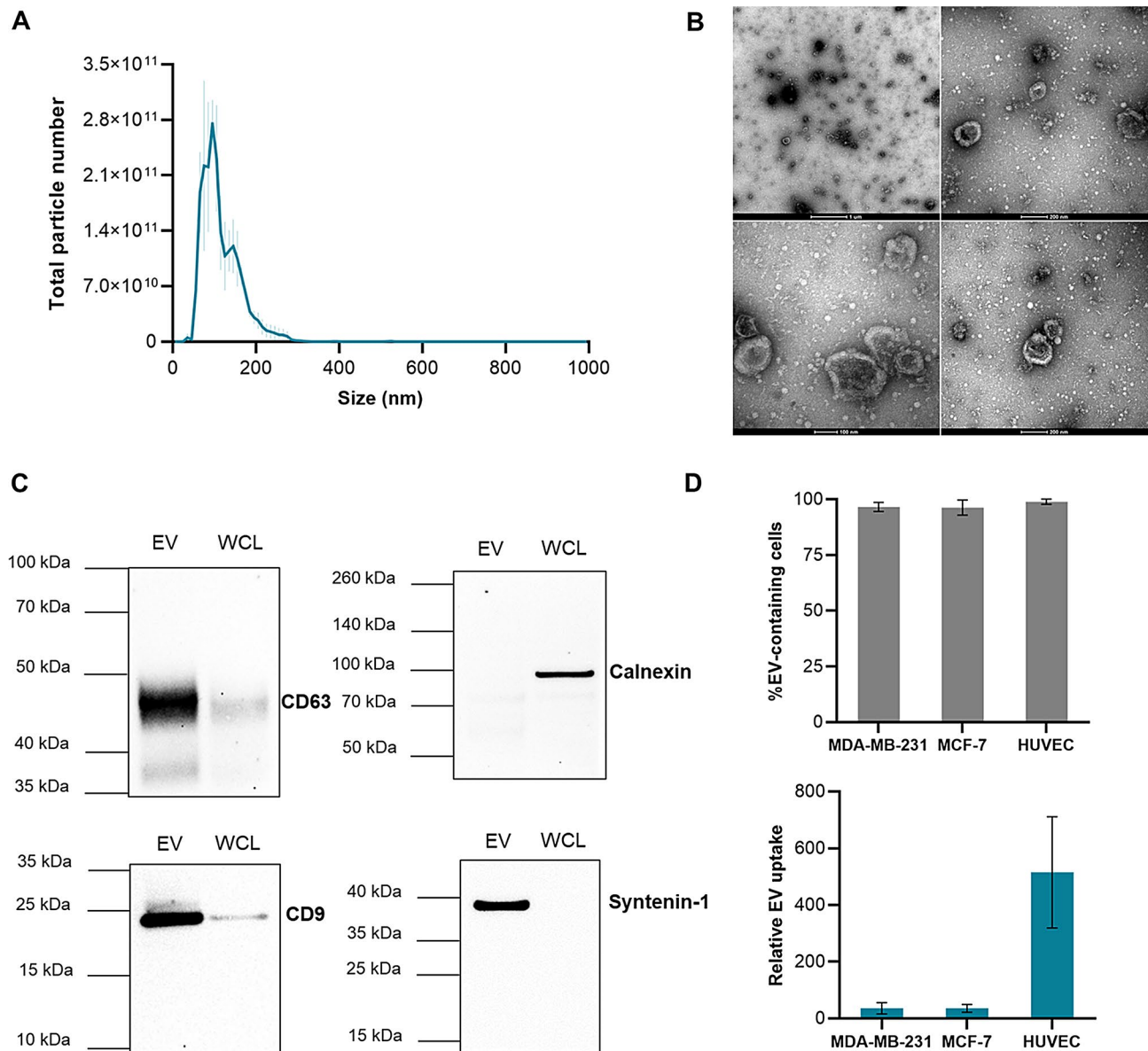


Fig. 5 Characterisation of EVs isolated from the MSC(WJ)-derived CM continuously produced in STR. **(A)** Size distribution profile of isolated MSC(WJ)-derived EVs obtained by NTA. Graph values are presented as mean ± SEM of 3 independent donors (n = 3). **(B)** Representative transmission electron microscopy images of isolated EVs after negative staining, at different magnifications. Scale bar: 1 μm (top left), 100 nm (bottom left), 200 nm (right). **(C)** Representative Western-blot images of positive EV markers CD63, CD9 and syntenin-1 and negative EV marker calnexin detection using isolated EV samples and the respective WCL of MSC(WJ). Full-length membrane/blot composites are presented in Supplementary Fig. 4. **(D)** Analysis of EV uptake by target cells (breast cancer cells MDA-MB-231, MCF-7 and HUVECs) after treatment with Alexa647-(red) labelled EVs. The percentage of EV-containing cells (top panel) and the relative EV uptake based on MFI values (ratio MFI of labelled-EV to MFI of free dye) (bottom panel) were determined by flow cytometry. Graph values are presented as mean ± SEM of 3 independent donors (n = 3). No statistically significant differences were found using a one-way ANOVA followed by a post-hoc Tukey's multiple comparisons test. EVs, extracellular vesicles; MSC(WJ), Wharton's jelly-derived mesenchymal stromal cells; CM, conditioned medium; NTA, nanoparticle tracking analysis; WCL, whole cell lysate; HUVECs, human umbilical vein endothelial cells; MFI, median fluorescence intensities

the use of S/XF chemically defined media as EV collection supplements [20, 22, 27]. While these formulations support cell viability, they are not completely free from particles, which can compromise EV manufacturing and the accurate characterization of their biochemical composition and function. Indeed, many EV collection

protocols rely on the use of basal culture medium during the cell conditioning stage for EV collection [21, 26, 48, 50, 57, 58], as it represents a more controlled and easier to implement option for minimizing external particle contamination. However, this approach may be too stringent for maintaining MSC fitness over 72 h, as it lacks

critical survival and adhesion factors. Preliminary studies from our group have shown that human MSC cultured in DMEM supplemented with EV-depleted hPL exhibited higher cell numbers and viability compared to basal DMEM, while yielding equivalent particle concentrations in the conditioned medium collected over three consecutive 24-hour batches (data not shown). This observation is consistent with other studies in the literature that demonstrate the beneficial role of EV-depleted hPL-based formulations and the stringency of basal media [59].

MSC(WJ) were expanded on Dissolvable microcarriers in a STR with intermittent agitation until maximum fold expansion using hPL-supplemented medium followed by EV production in stirred conditions using EV-depleted-hPL-supplemented medium. Both supplements are gamma irradiated as a pathogen reduction technology (PRT) formulation, which is essential to produce a safe MSC product for clinical use [60]. Similarly to our previous study using an alternative S/XF formulation [26], this new platform allowed MSC(WJ) adhesion to the microcarriers with an efficiency of $86 \pm 4.1\%$, which is notably higher than the typical $\leq 50\%$ efficiency reported for MSC(WJ) adhesion when using hPL-stirred cultures employing various microcarriers and agitation regimens [21, 38, 43, 61]. Additionally, taking advantage of the intermittent agitation and by increasing the total available microcarrier surface area by 50% in comparison to our previous protocol [26], a total number of $(6.0 \pm 0.18) \times 10^7$ cells was reached after 7 days, representing an approximate 30-fold cell expansion factor. This is higher than most values reported in the literature for MSC expansion in S/XF stirred culture conditions with similar or longer timeframes [20–22, 27, 28, 38, 43, 52, 61, 62]. The initial cell seeding density ($1,850 \text{ cell/cm}^2$) in the STR culture was intentionally lower than what is typically employed for S/XF microcarrier-based MSC expansion ($3,000\text{--}7,000 \text{ cells/cm}^2$) [20, 22, 43, 52, 53]. This reduction delayed the aggregation of cell-containing microcarriers throughout culture, a phenomenon accelerated by higher initial cell density per microcarrier [63]. Moreover, the homogeneous and full occupancy of the microcarriers was facilitated by incorporating static periods that promote MSC migration to empty microcarriers throughout culture, without signs of early bead aggregation [26, 63, 64]. The selected feeding strategy (i.e. STR operated under continuous fed-batch until day 4, followed by perfusion until day 7) facilitated efficient MSC(WJ) growth by maintaining optimal glucose and lactate levels, supporting previous findings that perfusion cultures achieve higher cell concentrations and superior fold expansion values compared to fed-batch strategies [28, 52]. Although a stationary growth phase was not observed, by day 7 the microcarriers were aggregated and nearly confluent, yielding a cell density of (5.6 ± 0.17)

$\times 10^4 \text{ cells/cm}^2$. To prevent cell detachment from microcarriers due to higher cell densities and aggregation [63], we started the EV production phase with MSC in a highly viable and proliferative state to minimize the impact of shear stress on cell viability during continuous stirred culture in EV-depleted hPL medium. For this stage, we selected a 3-day perfusion operation mode based on the initial observations of particle accumulation in the CM of MSC(WJ) cultured under static conditions for 72 h. Our results showed no particle accumulation over time, with total particle production being approximately 3 times higher when 24 h-medium renewal cycles were performed. These findings align with the work of Patel and colleagues [65], where mid-period collection of the CM led to an approximately 2-fold increase in MSC-EV production when compared to single collections at 6, 12 and 24 h. Additionally, studies on macrophage-derived CM showed similar EV concentrations at 24, 48, and 72 h, indicating no particle accumulation [66]. These findings suggest that EV production may function as a balanced intercellular communication system, where particle removal stimulates additional secretion - a phenomenon that continuous culture systems can exploit to improve EV yields. Indeed, during the 3-day EV continuous production stage in the STR, there were no significant differences in what concerns the total number of accumulated particles and the particle secretion rate by MSC(WJ) throughout time. Future experiments should compare EV collection on continuous *versus* batch-operation mode under identical culture conditions to directly assess the advantages of continuous harvesting in the STR system, as well as the bioequivalence of the EVs produced. Moreover, while a direct comparison with alternative bioreactor configurations was beyond the scope of this study, future studies could systematically evaluate various culture systems (e.g. hollow-fiber bioreactors, planar culture systems as multilayered flasks) under standardized conditions to better elucidate their relative advantages in terms of EV yield, cost-effectiveness and scalability.

To the best of our knowledge, this study is the first to establish a scalable culture system for the continuous collection of EVs produced from primary human MSC in a controlled STR. While alternative bioreactor platforms, such as hollow-fiber systems, have reported continuous EV production using perfusion techniques [49, 67, 68], these often rely on medium recirculation, contrasting to our approach which continuously harvests the EV-enriched CM. Importantly, a potential advantage of hollow-fiber bioreactors over STR for EV manufacturing could rely on their ability to mitigate the presence of exogenous EVs from medium supplements through the use of smaller membrane pore sizes [49, 68]. For instance, Garcia and colleagues used a 20 kDa pore size to guarantee EV retention and avoid the flowthrough of

serum-derived EVs to the isolated supernatants (i.e. cells cultured in the cartridge/extracapillary space) [68]. Our system tackles this contamination issue by using EV-depleted hPL, ensuring that only MSC-derived EVs accumulate in the conditioned medium.

Microcarrier-based stirred cultures of MSC have demonstrated significant increases in EV productivity compared to two-dimensional static cultures [20–24]. Besides causing significant intracellular pathways and expression alterations that regulate EV secretion, laminar or turbulent flow-induced shear stress leads to cell membrane tension and elongation, resulting in fragmentation and spontaneous self-assembly of vesicles [69]. Therefore, to further stimulate EV production, in this work, EV production was performed under continuous agitation at 60 rpm, which visually complied with the N_{Stu} criterion, that is the agitation speed that merely allows cell-laden microcarriers moving along the bottom of the microcarriers [70, 71]. Notably, during the 3-day continuous EV production stage, MSC(WJ) showed high viability and conventional cellular morphology while maintaining the cell number and particle production rate. This demonstrates that the EV-depleted hPL-supplemented culture medium and stirred culture conditions did not significantly compromise MSC(WJ) integrity. Moreover, at the end of culture, harvested MSC(WJ) presented the standard immunophenotype and trilineage differentiation potential, confirming that this EV production platform preserves MSC(WJ) cellular identity. These findings align with recent work reported by Lorenzini and colleagues, where MSC cultured for 3 successive periods of 72 h in medium supplemented with EV-depleted hPL maintained cell survival and cumulative EV production, a phenomenon not observed under standard starving conditions [59]. Future studies could further investigate the impact of various STR process parameters on EV secretion, including agitation regime [20], and conditioning stage duration, as well as other physiological stimuli such as oxygen tension, pH and temperature, all of which have been shown to influence EV production [72, 73].

After the upstream process, robust isolation methods are needed to efficiently process large volumes of CM. Many studies on MSC-EV production in scalable stirred systems still rely on polymer-based precipitation kits [21, 25, 28] and UC [20, 27], despite their limitations concerning scalability and low-purity grade EV samples [19, 33, 34, 74]. Tangential fluid filtration (TFF), alone or combined with chromatography, provides a scalable solution that efficiently processes large CM volumes, yielding high EV numbers with improved purity [35]. Haraszti and colleagues demonstrated that TFF improves the yield of MSC-EVs from CM of 3D stirred cultures by 7-fold compared to UC [23]. In another case, TFF coupled with SEC yielded approximately a 5.2-fold

increase in EV concentration when compared to density gradient UC after isolation of EVs from STR cultures of MSC(AT) [22]. The EV downstream platform presented herein builds upon previous work by our group, in which the combination of ultrafiltration, nuclease digestion and anion exchange chromatography (AEC) using the Capto™ Q ImpRes resin, successfully recovered 53% of MSC-EVs, while impurity levels complied with regulatory agency requirements [36]. Other groups have also reported the use of different AEC columns to isolate EVs from the CM of MSC [75–77] and other cell lines [78, 79]. By incorporating TFF for the concentration/diafiltration step in the present work, we successfully established a large-scale EV isolation protocol capable of processing substantial CM volumes (above 600 mL) and yielding high purity EVs in large numbers within 12 h.

The particle yield factor, which depends on both upstream and downstream processes, is an important metric for comparing EV manufacturing platforms [45]. Our integrated process yielded a factor of $(1.21 \pm 0.31) \times 10^4$ particles/cell/day, surpassing those reported by others. For instance, the use of a 0.1 L vertical-wheel system and UC for EV isolation, resulted in a particle yield factor ranging around $0.5\text{--}2.5 \times 10^3$ particles/cell/day, depending on the agitation speed applied [20]. Additionally, MSC(AT) cultures processed with TFF-SEC yielded approximately 2.25×10^3 particles/cell/day and 6.65×10^3 particles/cell/day, when using static planar flasks and a 0.2 L STR, respectively [22].

Notably, our platform generated a total of $(1.92 \pm 0.38) \times 10^{12}$ EVs, which is clinically relevant considering that the therapeutic doses of MSC-EVs range from 10^{10} to 10^{11} per administration [18] (i.e. representing the production of 10 EV doses). Moreover, the established system is easily scalable and potentially capable of producing enough EV doses for an entire clinical trial from a single production batch, which represents a key advantage in terms of standardization by facilitating quality control.

Importantly, the isolated particles exhibited characteristics consistent with those typically associated to MSC-EVs. They presented a homogeneous small-size distribution with a mean diameter of around 116 nm and displayed a cup-shaped morphology in TEM images, consistent with previous studies [20, 22, 26, 28]. The slightly lower negative surface charge of the isolated MSC-EVs (-23.4 ± 6.23 mV) compared to other studies [43, 57] could be related to the selected isolation method, which separates EVs from the contaminants based on their negative charge. The isolation process yielded EV samples with a PPR of $(5.53 \pm 1.55) \times 10^9$ particles/ μg , which is higher than other EV preparations obtained from CM using other isolation methods [20, 21, 23, 28, 58], suggesting superior EV purity. For instance, EVs isolated from the CM of MSC cultured under stirred

conditions had a PPR of 0.9×10^9 and 1.23×10^9 particles/ μg when using UC and TFF, respectively [23]. Moreover, the detection of tetraspanins CD9 and CD63 and syn-tenin-1 at higher levels in isolated EV samples compared to WCL controls further confirmed EV enrichment and purity of the preparation. Finally, HUVECs and breast cancer cell lines readily internalised the isolated MSC-EVs, validating their potential application as natural therapeutics or drug delivery vehicles.

Further studies are needed to better characterize and evaluate the therapeutic potential of MSC-EVs generated using our manufacturing platform. These should include transcriptomic and proteomic analyses of MSC-EV molecular cargo [80, 81], as well as *in vitro* and *in vivo* functional studies to assess EV potency [82], including their hematopoietic support [83, 84], immunomodulatory [85, 86], and proangiogenic activities [22, 87]. Additionally, the potential use of MSC-EVs as drug delivery vehicles could be explored [17], leveraging their inherent tissue-targeting capabilities.

Ultimately, the significant capital investment and high cost of goods (COG) associated with MSC and MSC-EV manufacturing pose considerable obstacles to the widespread adoption of MSC-based therapies. Overcoming these challenges requires a thorough assessment of their economic feasibility to ensure these therapies can be both successful and accessible to a larger patient population [88].

Conclusion

In this work, we successfully developed a fully scalable platform for the clinical-scale manufacturing of MSC-EVs, integrating GMP-compliant upstream and downstream processes. To the best of our knowledge, this is the first study to establish a robust S/XF system for the continuous collection of MSC(WJ)-derived EVs using a controlled STR. By optimizing critical parameters such as cell seeding density per microcarrier surface area and agitation regimen, our system achieved a remarkable ~ 30 -fold expansion of MSC(WJ) in 7 days - a significant improvement over most reported values for similar systems and timeframes. MSC expansion was followed by a 3-day continuous EV production stage under stirred conditions using a novel EV-depleted hPL-supplement, which did not compromise cell viability and identity of MSC. For EV isolation, TFF was coupled with AEC, enabling the efficient processing of large CM volumes (over 600 mL) and yielding high-purity EVs in substantial numbers. The MSC-EVs produced exhibited all the expected characteristics, including size, surface charge, morphology, protein markers and effective target cell internalisation. Our platform demonstrated a particle yield factor of approximately 1.2×10^4 particles/cell/day, allowing for the reproducible, high-yield manufacturing

of clinically relevant quantities of MSC-EVs. This represents a significant step towards making MSC-EV-based therapies both economically viable and widely available in routine clinical practice. Future research should prioritize functional assays to evaluate the therapeutic potential of MSC-EVs in different contexts, while also optimizing the platform to achieve higher yields and improved process efficiency.

Abbreviations

A/A	Antibiotic-antimycotic
AEC	Anion exchange chromatography
CM	Conditioned medium
CV	Column volumes
DAPI	4',6-diamidino-2-phenylindole
DMEM	Dulbecco's modified Eagle's medium
EVs	Extracellular vesicles
FBS	Fetal bovine serum
GI	Gamma-irradiated
GMP	Good manufacturing practices
hPL	Human platelet lysate
HUVECs	Human umbilical vein endothelial cells
ISCT	International Society for Cell and Gene Therapy
MFI	Median fluorescence intensity
MSC(WJ)	Wharton's jelly-derived mesenchymal stromal cells
MSC	Mesenchymal stromal cells
MSC-EVs	Mesenchymal-stromal-cell-derived extracellular vesicles
NTA	Nanoparticle tracking analysis
PBS	Phosphate-buffered saline
PPR	Particle-to-protein ratio
S/XF	Serum-/xeno(genic)-free
SEC	Size-exclusion chromatography
STR	Stirred tank reactor
TBST	Tris-buffered saline with tween
TEM	Transmission electron microscopy
TFF	Tangential flow filtration
UC	Ultracentrifugation
WCL	Whole cell lysate

Supplementary Information

The online version contains supplementary material available at <https://doi.org/10.1186/s13287-025-04341-2>.

Supplementary Material 1

Acknowledgements

The authors acknowledge Corning for providing the Dissolvable microcarriers. The authors would like to thank the Electron Microscopy Facility of Instituto Gulbenkian de Ciéncia (IGC), Oeiras, Portugal, for their assistance with transmission electron microscopy analysis. The authors declare that they have not use AI-generated work in this manuscript.

Author contributions

CSU, AFP, GAM and CLS conceptualised the research study. CSU performed the experiments and further analysis. WS and TFM performed experiments. AFP, CR and JC supported the establishment of the stirred-tank reactor system. M-CH, Y-HL and H-TL supported the use of human platelet lysate supplements for cell expansion and EV production. CSU, GAM, and CLS discussed the results and wrote the manuscript. All authors revised the manuscript and approved the final version. AFP, JC and CLS provided financial support.

Funding

This work was financed by national funds from FCT—Fundação para a Ciéncia e a Tecnologia, I.P., within the scope of the projects UIDB/04565/2020 and UIDP/04565/2020 of the Research Unit Institute for Bioengineering and Biosciences—iBB and the project LA/P/0140/2020 of the Associate Laboratory

Institute for Health and Bioeconomy—i4HB, and through the project PTDC/EQU-EQU/31651/2017. CSU acknowledges FCT for the PhD grant PD/BD/150336/2019.

Data availability

All data generated for this study is included in the article/supplementary material. Further inquiries can be directed to the corresponding author.

Declarations

Ethics approval and consent to participate

For primary cell isolation (MSC(WJ)), human samples were obtained from healthy donors at Hospital São Francisco Xavier, Centro Hospitalar de Lisboa Ocidental (CHLO) after written and informed consent and according to the Directive 2004/23/EC of the European Parliament and of the Council of 31 March 2004 on setting standards of quality and safety for the donation, procurement, testing, processing, preservation, storage and distribution of human tissues and cells (Portuguese Law 22/2007, June 29). The collaborative project Protocol iBB/SGO-CHLO (iBB-Institute for Bioengineering and Biosciences of Instituto Superior Técnico and Department of Gynecology and Obstetrics (SGO, Serviço de Ginecologia e Obstetrícia) of CHLO) was approved on May 2012 by the Ethics Committee of CHLO - n°1277. The cell lines used in this study are commercially available and were provided in accordance with the vendors' compliance policies. HUVECs were obtained from Lonza and the breast cancer cell lines MDA-MB-231 and MCF-7 were obtained from ATCC.

Consent for publication

N/A.

Competing interests

M-CH, Y-HL and H-TL had compensated employment at AventaCell BioMedical Corp. No potential conflicts of interest were disclosed by the other authors.

Author details

¹Department of Bioengineering and iBB - Institute for Bioengineering and Biosciences at Instituto Superior Técnico, Universidade de Lisboa, Lisboa, Portugal

²Associate Laboratory i4HB - Institute for Health and Bioeconomy at Instituto Superior Técnico, Universidade de Lisboa, Lisboa, Portugal

³AventaCell BioMedical Corp, Kent, WA, USA

Received: 15 November 2024 / Accepted: 11 April 2025

Published online: 24 April 2025

References

- van Niel G, D'Angelo G, Raposo G. Shedding light on the cell biology of extracellular vesicles. *Nat Rev Mol Cell Biol*. 2018;19:213–28. <https://doi.org/10.1038/NRM.2017.125>.
- Johnstone RM, Mathew A, Mason AB, Teng K. Exosome formation during maturation of mammalian and avian reticulocytes: evidence that exosome release is a major route for externalization of obsolete membrane proteins. *J Cell Physiol*. 1991;147:27–36. <https://doi.org/10.1002/JCP.1041470105>.
- Elsharkasy OM, Nordin JZ, Hagey DW, de Jong OG, Schifferles RM, Andaloussi S et al. Extracellular vesicles as drug delivery systems: why and how? *Adv Drug Deliv Rev*. 2020;159:332–43. <https://doi.org/10.1016/J.ADDR.2020.04.004>.
- Roy S, Hochberg FH, Jones PS. Extracellular vesicles: the growth as diagnostics and therapeutics; a survey. *J Extracell Vesicles*. 2018;7. <https://doi.org/10.1080/20013078.2018.1438720>.
- Saleh AF, Lázaro-Ibáñez E, Forsgard MAM, Shatnyeva O, Osteikoetxea X, Karlsson F, et al. Extracellular vesicles induce minimal hepatotoxicity and immunogenicity. *Nanoscale*. 2019;11:6990–7001. <https://doi.org/10.1039/C8NR08720B>.
- Kou M, Huang L, Yang J, Chiang Z, Chen S, Liu J, et al. Mesenchymal stem cell-derived extracellular vesicles for immunomodulation and regeneration: a next generation therapeutic tool? *Cell Death Disease*. 2022;13:7. <https://doi.org/10.1038/s41419-022-05034-x>.
- Phinney DG, Pittenger MF. Concise review: MSC-Derived exosomes for Cell-Free therapy. *Stem Cells*. 2017;35:851–8. <https://doi.org/10.1002/stem.2575>.
- Doepfner TR, Herz J, Görgens A, Schlechter J, Ludwig A-K, Radtke S, et al. *Stem Cells Transl Med*. 2015;4:1131–43. Extracellular Vesicles Improve Post-Stroke Neuroregeneration and Prevent Postischemic Immunosuppression. <https://doi.org/10.5966/sctm.2015-0078>
- Gatti S, Bruno S, Deregibus MC, Sordi A, Cantaluppi V, Tetta C, et al. Microvesicles derived from human adult mesenchymal stem cells protect against ischaemia-reperfusion-induced acute and chronic kidney injury. *Nephrol Dialysis Transplantation*. 2011;26:1474–83. <https://doi.org/10.1093/ndt/gfr015>.
- Levy O, Kuai R, Siren EMJ, Bhore D, Milton Y, Nissar N et al. Shattering barriers toward clinically meaningful MSC therapies. *Sci Adv* 2020;6. <https://doi.org/10.1126/sciadv.aba6884>
- Viswanathan S, Ciccocioppo R, Galipeau J, Krampera M, Le Blanc K, Martin I, et al. Consensus international Council for commonality in blood banking Automation—International society for cell & gene therapy statement on standard nomenclature abbreviations for the tissue of origin of mesenchymal stromal cells. *Cytotherapy*. 2021;23:1060–3. <https://doi.org/10.1016/J.JCYT.2021.04.009>.
- Alofisel| European Medicines Agency. n.d. <https://www.ema.europa.eu/en/medicines/human/EPAR/alofisel> (accessed February 12, 2023).
- Jeong JO, Han JW, Kim JM, Cho HJ, Park C, Lee N, et al. Malignant tumor formation after transplantation of short-term cultured bone marrow mesenchymal stem cells in experimental myocardial infarction and diabetic neuropathy. *Circ Res*. 2011;108:1340–7. <https://doi.org/10.1161/CIRCRESAHA.110.239848>.
- Wang S, Guo L, Ge J, Yu L, Cai T, Tian R, et al. Excess integrins cause lung entrapment of mesenchymal stem cells. *Stem Cells*. 2015;33:3315–26. <https://doi.org/10.1002/STEM.2087>.
- Bahr MM, Amer MS, Abo-El-Sooud K, Abdallah AN, El-Tookey OS. Preservation techniques of stem cells extracellular vesicles: a gate for manufacturing of clinical grade therapeutic extracellular vesicles and long-term clinical trials. *Int J Vet Sci Med*. 2020;8:1–8. <https://doi.org/10.1080/23144599.2019.1704992>.
- Ridzuan N, Zakaria N, Widera D, Sheard J, Morimoto M, Kiyokawa H, et al. Human umbilical cord mesenchymal stem cell-derived extracellular vesicles ameliorate airway inflammation in a rat model of chronic obstructive pulmonary disease (COPD). *Stem Cell Res Ther*. 2021;12. <https://doi.org/10.1186/s13287-020-02088-6>.
- Ulpiano C, da Silva CL, Monteiro GA. Bioengineered Mesenchymal-Stromal-Cell-Derived extracellular vesicles as an improved drug delivery system: methods and applications. *Biomedicines* 2023;11. <https://doi.org/10.3390/biomedicines11041231>
- Lotfy A, Abo-Quella NM, Wang H. Mesenchymal stromal/stem cell (MSC)-derived exosomes in clinical trials. *Stem Cell Res Ther*. 2023;14:66. <https://doi.org/10.1186/s13287-023-03287-7>.
- Pincela Lins PM, Pirllet E, Szymonik M, Bronckaers A, Nelissen I. Manufacture of extracellular vesicles derived from mesenchymal stromal cells. *Trends Biotechnol*. 2023;41:965–81. <https://doi.org/10.1016/J.TIBTECH.2023.01.003>.
- Jeske R, Liu C, Duke L, Canonico Castro ML, Muok L, Arthur P, et al. Upscaling human mesenchymal stromal cell production in a novel vertical-wheel bioreactor enhances extracellular vesicle secretion and cargo profile. *Bioact Mater*. 2023;25:732–47. <https://doi.org/10.1016/j.bioactmat.2022.07.004>.
- de Almeida Fuzeta M, Bernardes N, Oliveira FD, Costa AC, Fernandes-Platzgummer A, Farinha JP, et al. Scalable production of human mesenchymal stromal Cell-Derived extracellular vesicles under Serum-/Xeno-Free conditions in a Microcarrier-Based bioreactor culture system. *Front Cell Dev Biol*. 2020;8. <https://doi.org/10.3389/fcell.2020.553444>.
- Costa MHG, Costa MS, Painho B, Sousa CD, Carrondo I, Oltra E, et al. Enhanced bioprocess control to advance the manufacture of mesenchymal stromal cell-derived extracellular vesicles in stirred-tank bioreactors. *Biotechnol Bioeng*. 2023;120:2725–41. <https://doi.org/10.1002/bit.28378>.
- Haraszti RA, Miller R, Stoppato M, Sere YY, Coles A, Didiot MC, et al. Exosomes produced from 3D cultures of MSCs by tangential flow filtration show higher yield and improved activity. *Mol Ther*. 2018;26:2838. <https://doi.org/10.1016/J.YMTHE.2018.09.015>.
- Barekzai J, Friedrich J, Okpara M, Refflinghaus L, Eckhardt D, Czermak P, et al. Dynamic expansion of mesenchymal stem/stromal cells in a stirred tank bioreactor promotes the release of potent extracellular vesicles. *AIMS Bioeng*. 2023;10:240–64. <https://doi.org/10.3934/bioeng.2023016>.
- Xu C, Zhao J, Li Q, Hou L, Wang Y, Li S, et al. Exosomes derived from three-dimensional cultured human umbilical cord mesenchymal stem cells

- ameliorate pulmonary fibrosis in a mouse silicosis model. *Stem Cell Res Ther.* 2020;11:1–12. <https://doi.org/10.1186/S13287-020-02023-9/FIGURES/7>.
26. Bandarra-Tavares H, Franchi-Mendes T, Ulpiano C, Morini S, Kaur N, Harris-Becker A et al. Dual production of human mesenchymal stromal cells and derived extracellular vesicles in a dissolvable microcarrier-based stirred culture system. *Cytotherapy* 2024;1–8. <https://doi.org/10.1016/j.jcyt.2024.03.01>
 27. Jalilian E, Massoumi H, Bigit B, Amin S, Katz EA, Guaiquil VH, et al. Bone marrow mesenchymal stromal cells in a 3D system produce higher concentration of extracellular vesicles (EVs) with increased complexity and enhanced neuronal growth properties. *Stem Cell Res Ther.* 2022;13:1–13. <https://doi.org/10.1186/S13287-022-03128-Z/FIGURES/5>.
 28. Fernandes-Platzgummer A, Cunha R, Morini S, Carvalho M, Moreno-Cid J, Cabral J, et al. Optimized operation of a controlled stirred tank reactor system for the production of mesenchymal stromal cells and their extracellular vesicles. *Biotechnol Bioeng.* 2023;120:2742–55. <https://doi.org/10.22541/au.167160787.74320022/v1>.
 29. Haraszti RA, Miller R, Stoppato M, Sere YY, Coles A, Didiot MC, et al. Exosomes produced from 3D cultures of MSCs by tangential flow filtration show higher yield and improved activity. *Mol Ther.* 2018;26:2838–47. <https://doi.org/10.1016/j.jymthe.2018.09.015>.
 30. Adlerz K, Patel D, Rowley J, Ng K, Ahsan T. Strategies for scalable manufacturing and translation of MSC-derived extracellular vesicles. *Stem Cell Res.* 2020;48. <https://doi.org/10.1016/j.scr.2020.101978>.
 31. Shelke GV, Lä Sser C, Gho YS, Lö Tvall J, Lö J. Importance of exosome depletion protocols to eliminate functional and RNA-containing extracellular vesicles from fetal bovine serum. *J Extracell Vesicles.* 2014;3. <https://doi.org/10.3402/jev.v3.24783>.
 32. van Balkom BWM, Gremmels H, Giebel B, Lim SK. Proteomic signature of mesenchymal stromal Cell-Derived small extracellular vesicles. *Proteomics.* 2019;19:1800163. <https://doi.org/10.1002/PMIC.201800163>.
 33. Webber J, Clayton A. How pure are your vesicles? *J Extracell Vesicles.* 2013. <https://doi.org/10.3402/JEV.V2I0.19861.2>.
 34. Williams S, Jalal AR, Lewis MP, Davies OG. A survey to evaluate parameters governing the selection and application of extracellular vesicle isolation methods. *J Tissue Eng.* 2023;14. <https://doi.org/10.1177/20417314231155114>.
 35. Liangsupree T, Multia E, Riekkola ML. Modern isolation and separation techniques for extracellular vesicles. *J Chromatogr A.* 2021;1636. <https://doi.org/10.1016/j.chroma.2020.461773>.
 36. Silva RM, Rosa SS, Cunha R, da Silva L, Azevedo C, Fernandes-Platzgummer AM. Anion exchange chromatography-based platform for the scalable purification of extracellular vesicles derived from human mesenchymal stromal cells. *Sep Purif Technol.* 2023;310. <https://doi.org/10.1016/j.seppur.2023.123238>.
 37. Benedikter BJ, Bouwman FG, Vajen T, Heinzmann ACA, Grauls G, Mariman EC et al. Ultrafiltration combined with size exclusion chromatography efficiently isolates extracellular vesicles from cell culture media for compositional and functional studies. *Sci Rep* 2017;7. <https://doi.org/10.1038/s41598-017-15717-7>
 38. de Soure AM, Fernandes-Platzgummer A, Moreira F, Lilaia C, Liu S-H, Ku C-P, et al. Integrated culture platform based on a human platelet lysate supplement for the isolation and scalable manufacturing of umbilical cord matrix-derived mesenchymal stem/stromal cells. *J Tissue Eng Regen Med.* 2017;11:1630–40. <https://doi.org/10.1002/term.2200>.
 39. Dominici M, Le Blanc K, Mueller I, Slaper-Cortenbach I, Marini FC, Krause DS, et al. Minimal criteria for defining multipotent mesenchymal stromal cells. The international society for cellular therapy position statement. *Cytotherapy.* 2006;8:315–7. <https://doi.org/10.1080/14653240600855905>.
 40. Santos F, Dos, Andrade PZ, Abecasis MM, Gimble JM, Chase LG, Campbell AM, et al. Toward a clinical-grade expansion of mesenchymal stem cells from human sources: A microcarrier-based culture system under xeno-free conditions. *Tissue Eng Part C Methods.* 2011;17:1201–10. <https://doi.org/10.1089/ten.tec.2011.0255>.
 41. Schop D, Janssen FW, Van Rijn LDS, Fernandes H, Bloem RM, De Bruijn JD, et al. Growth, metabolism, and growth inhibitors of mesenchymal stem cells. *Tissue Eng Part A.* 2009;15:1877–86. <https://doi.org/10.1089/TEN.TEA.2008.0345>.
 42. Dos Santos F, Campbell A, Fernandes-Platzgummer A, Andrade PZ, Gimble JM, Wen Y, et al. A xenogeneic-free bioreactor system for the clinical-scale expansion of human mesenchymal stem/stromal cells. *Biotechnol Bioeng.* 2014;111:1116–27. <https://doi.org/10.1002/bit.25187>.
 43. de Sousa Pinto D, Bandejas C, de Almeida Fuzeta M, Rodrigues CAV, Jung S, Hashimura Y, et al. Scalable manufacturing of human mesenchymal stromal cells in the Vertical-Wheel bioreactor system: an experimental and economic approach. *Biotechnol J.* 2019;14. <https://doi.org/10.1002/biot.201800716>.
 44. Théry C, Witwer KW, Aikawa E, Alcaraz MJ, Anderson JD, Andriantsitohaina R, et al. Minimal information for studies of extracellular vesicles 2018 (MISEV2018): a position statement of the international society for extracellular vesicles and update of the MISEV2014 guidelines. *J Extracell Vesicles.* 2018;7. <https://doi.org/10.1080/20013078.2018.1535750>.
 45. Grangier A, Branchu J, Volatron J, Piffoux M, Gazeau F, Wilhelm C, et al. Technological advances towards extracellular vesicles mass production. *Adv Drug Deliv Rev.* 2021;176. <https://doi.org/10.1016/j.addr.2021.113843>.
 46. Chuo STY, Chien JCY, Lai CPK. Imaging extracellular vesicles: current and emerging methods. *J Biomed Sci.* 2018;25. <https://doi.org/10.1186/S12929-018-0494-5>.
 47. Sarvar DP, Shamsasenjan K, Akbarzadehlaleh P. Mesenchymal stem cell-derived exosomes: new opportunity in cell-free therapy. *Adv Pharm Bull.* 2016;6:293–9. <https://doi.org/10.15171/apb.2016.041>.
 48. Andriolo G, Provasi E, Lo Cicero V, Brambilla A, Soncin S, Torre T, et al. Exosomes from human cardiac progenitor cells for therapeutic applications: development of a GMP-grade manufacturing method. *Front Physiol.* 2018;9. <https://doi.org/10.3389/fphys.2018.01169/FULL>.
 49. Gobin J, Muradia G, Mehic J, Westwood C, Couvrette L, Stalker A, et al. Hollow-fiber bioreactor production of extracellular vesicles from human bone marrow mesenchymal stromal cells yields nanovesicles that mirrors the immuno-modulatory antigenic signature of the producer cell. *Stem Cell Res Ther.* 2021;12. <https://doi.org/10.1186/s13287-021-02190-3>.
 50. dos Santos NCD, Bruzadelle-Vieira P, de Cássia Noronha N, Mizukami-Martins A, Orellana MD, Bentley MVLB, et al. Transitioning from static to suspension culture system for large-scale production of xeno-free extracellular vesicles derived from mesenchymal stromal cells. *Biotechnol Prog.* 2024;40:e3419. <https://doi.org/10.1002/BTPR.3419>.
 51. Mizukami A, Fernandes-Platzgummer A, Carmelo JG, Swiech K, Covas DT, Cabral JMS, et al. Stirred tank bioreactor culture combined with serum-/xenogeneic-free culture medium enables an efficient expansion of umbilical cord-derived mesenchymal stem/stromal cells. *Biotechnol J.* 2016;11:1048–59. <https://doi.org/10.1002/biot.201500532>.
 52. Cunha B, Aguiar T, Silva MM, Silva RJS, Sousa MFQ, Pineda E, et al. Exploring continuous and integrated strategies for the up- and downstream processing of human mesenchymal stem cells. *J Biotechnol.* 2015;213:97–108. <https://doi.org/10.1016/j.jbiotec.2015.02.023>.
 53. Heathman TRJ, Nienow AW, Rafiq QA, Coopman K, Kara B, Hewitt CJ. Agitation and aeration of stirred-bioreactors for the microcarrier culture of human mesenchymal stem cells and potential implications for large-scale bioprocess development. *Biochem Eng J.* 2018;136:9–17. <https://doi.org/10.1016/j.bej.2018.04.011>.
 54. Kuan-liang Chen A, Kong Chew Y, Tan HY, Reuveny S, Kah Weng SO. Increasing efficiency of human mesenchymal stromal cell culture by optimization of microcarrier concentration and design of medium feed. *Cytotherapy* 2015;17. <https://doi.org/10.1016/j.jcyt.2014.08.011>
 55. Mastrogiacomo M, Brini AT, Visai L, De Girolamo L, Swiech K. Successful use of human AB serum to support the expansion of adipose Tissue-Derived mesenchymal stem/stromal cell in a Microcarrier-Based platform. *Front Bioeng Biotechnol* 2020;8. <https://doi.org/10.3389/fbioe.2020.00307>
 56. Tozzetti PA, Caruso SR, Mizukami A, Fernandes TR, da Silva FB, Traina F, et al. Expansion strategies for human mesenchymal stromal cells culture under xeno-free conditions. *Biotechnol Prog.* 2017;33:1358–67. <https://doi.org/10.1002/BTPR.2494>.
 57. Wright A, Snyder O, He H, Christenson LK, Fleming S, Weiss ML. Procoagulant activity of umbilical Cord-Derived mesenchymal stromal cells' extracellular vesicles (MSC-EVs). *Int J Mol Sci.* 2023;24:9216. <https://doi.org/10.3390/IJMS24119216/S1>.
 58. Görgens A, Corso G, Hagey DW, Jawad Wiklander R, Gustafsson MO, Felldin U, et al. Identification of storage conditions stabilizing extracellular vesicles preparations. *J Extracell Vesicles.* 2022;11. <https://doi.org/10.1002/JEV2.12238>.
 59. Lorenzini B, Peltzer J, Goulinet S, Rival B, Lataillade JJ, Uzan G, et al. Producing vesicle-free cell culture additive for human cells extracellular vesicles manufacturing. *J Controlled Release.* 2023;355:501–14. <https://doi.org/10.1016/j.jconrel.2023.01.073>.
 60. Bieback K, Fernandez-Muñoz B, Pati S, Schäfer R. Gaps in the knowledge of human platelet lysate as a cell culture supplement for cell therapy: a joint publication from the AABB and the international society for cell & gene

- therapy. *Cytotherapy*. 2019;21:911–24. <https://doi.org/10.1016/j.jcyt.2019.06.06>.
61. Sion C, Loubière C, Wlodarczyk-Biegun MK, Davoudi N, Müller-Renno C, Guedon E et al. Effects of microcarriers addition and mixing on WJ-MSC culture in bioreactors. *Biochem Eng J* 2020;157. <https://doi.org/10.1016/j.bej.2020.107521>
 62. Petry F, Smith JR, Leber J, Salz D, Czermak P, Weiss ML. Manufacturing of human umbilical cord mesenchymal stromal cells on microcarriers in a dynamic system for clinical use. *Stem Cells Int*. 2016. <https://doi.org/10.1155/2016/4834616>.
 63. Ferrari C, Balandras F, Guedon E, Olmos E, Chevalot I, Marc A. Limiting cell aggregation during mesenchymal stem cell expansion on microcarriers. *Biotechnol Prog*. 2012;28:780–7. <https://doi.org/10.1002/btpr.1527>.
 64. Chen S, Sato Y, Tada Y, Suzuki Y, Takahashi R, Okanojo M, et al. Facile bead-to-bead cell-transfer method for serial subculture and large-scale expansion of human mesenchymal stem cells in bioreactors. *Stem Cells Transl Med*. 2021;10:1329–42. <https://doi.org/10.1002/sctm.20-0501>.
 65. Patel DB, Gray KM, Santharam Y, Lamichhane TN, Stroka KM, Jay SM. Impact of cell culture parameters on production and vascularization bioactivity of mesenchymal stem cell-derived extracellular vesicles. *Bioeng Transl Med*. 2017;2:170–9. <https://doi.org/10.1002/btm2.10065>.
 66. Arteaga-Blanco LA, Mojoli A, Monteiro RQ, Sandim V, Menna-Barreto S, Santos Pereira-Dutra RF. Characterization and internalization of small extracellular vesicles released by human primary macrophages derived from Circulating monocytes. *PLoS ONE*. 2020;15. <https://doi.org/10.1371/journal.pone.0237795>.
 67. St-Denis-Bissonnette F, Cummings SE, Qiu S, Stalker A, Muradia G, Mehic J, et al. A clinically relevant large-scale biomanufacturing workflow to produce natural killer cells and natural killer cell-derived extracellular vesicles for cancer immunotherapy. *J Extracell Vesicles*. 2023;12:e12387. <https://doi.org/10.1002/jev2.12387>.
 68. García SG, Sanroque-Muñoz M, Clos-Sansalvador M, Font-Morón M, Monguió-Tortajada M, Borràs FE et al. Hollow fiber bioreactor allows sustained production of immortalized mesenchymal stromal cell-derived extracellular vesicles. *Extracell Vesicles Circ Nucleic Acids*. 2024;5:201–20 2024;5:201–20. <https://doi.org/10.20517/EVCNA.2023.76>
 69. Thone MN, Kwon YJ. Extracellular blebs: Artificially-induced extracellular vesicles for facile production and clinical translation. *Methods*. 2020;177:135–45. <https://doi.org/10.1016/j.jymeth.2019.11.007>.
 70. Jossen V, Schirmer C, Mostafa Sindi D, Eibl R, Kraume M, Pörtner R et al. Theoretical and practical issues that are relevant when scaling up hMSC microcarrier production processes. *Stem Cells Int* 2016;2016. <https://doi.org/10.1155/2016/4760414>
 71. Tsai AC, Jeske R, Chen X, Yuan X, Li Y. Influence of microenvironment on mesenchymal stem cell therapeutic potency: from planar culture to microcarriers. *Front Bioeng Biotechnol*. 2020;8. <https://doi.org/10.3389/fbioe.2020.00640>.
 72. Tse SW, Tan CF, Park JE, Gnanasekaran J, Gupta N, Low JK et al. Microenvironmental Hypoxia Induces Dynamic Changes in Lung Cancer Synthesis and Secretion of Extracellular Vesicles. *Cancers* 2020, Vol 12, Page 2917. 2020;12:2917. <https://doi.org/10.3390/CANCERS12102917>
 73. Gong C, Zhang X, Shi M, Li F, Wang S, Wang Y, et al. Tumor exosomes reprogrammed by low pH are efficient targeting vehicles for smart drug delivery and personalized therapy against their homologous tumor. *Adv Sci*. 2021;8:2002787. <https://doi.org/10.1002/ADVS.202002787>.
 74. Paolini L, Zandrini A, Noto G, Di, Busatto S, Lottini E, Radeghieri A, et al. Residual matrix from different separation techniques impacts exosome biological activity. *Sci Rep*. 2016;6. <https://doi.org/10.1038/SREP23550>.
 75. Shigemoto-Kuroda T, Oh JY, Kim Dki, Jeong HJ, Park SY, Lee HJ, et al. MSC-derived extracellular vesicles attenuate immune responses in two autoimmune murine models: type 1 diabetes and uveoretinitis. *Stem Cell Rep*. 2017;8:1214–25. <https://doi.org/10.1016/J.STEMCR.2017.04.008>.
 76. Kim DK, Nishida H, An SY, Shetty AK, Bartosh TJ, Prockop DJ. Chromatographically isolated CD63 + CD81 + extracellular vesicles from mesenchymal stromal cells rescue cognitive impairments after TBI. *Proc Natl Acad Sci U S A*. 2015;113:170–5. https://doi.org/10.1073/PNAS.1522297113/SUPPL_FILE/PNAS.201522297SI.PDF.
 77. Pacienza N, Lee RH, Bae EH, Kim D, ki, Liu Q, Prockop DJ, et al. In vitro macrophage assay predicts the in vivo Anti-inflammatory potential of exosomes from human mesenchymal stromal cells. *Mol Ther Methods Clin Dev*. 2019;13:67–76. <https://doi.org/10.1016/J.OMTM.2018.12.003>.
 78. Heath N, Grant L, De Oliveira TM, Rowlinson R, Osteoetxea X, Dekker N, et al. Rapid isolation and enrichment of extracellular vesicle preparations using anion exchange chromatography. *Sci Rep* 2018. 2018;8:1. <https://doi.org/10.1038/s41598-018-24163-y>.
 79. Seo N, Nakamura J, Kaneda T, Tateno H, Shimoda A, Ichiki T, et al. Distinguishing functional exosomes and other extracellular vesicles as a nucleic acid cargo by the anion-exchange method. *J Extracell Vesicles*. 2022;11. <https://doi.org/10.1002/JEV2.12205>.
 80. Yu D, Mei Y, Wang L, Zhao Y, Fan X, Liang D, et al. Nano-seq analysis reveals different functional tendency between exosomes and microvesicles derived from hUMSC. *Stem Cell Res Ther*. 2023;14. <https://doi.org/10.1186/s13287-023-03491-5>.
 81. Wang Zgang, He Z yi, Liang S, Yang Q, Cheng P, Chen A. min. Comprehensive proteomic analysis of exosomes derived from human bone marrow, adipose tissue, and umbilical cord mesenchymal stem cells. *Stem Cell Res Ther* 2020;11. <https://doi.org/10.1186/s13287-020-02032-8>
 82. Nguyen VVT, Witwer KW, Verhaar MC, Strunk D, Van Bas WM et al. Functional assays to assess the therapeutic potential of extracellular vesicles 2020. <https://doi.org/10.1002/jev2.12033>
 83. Bucar S, Branco AD, de Mata M, Milhano MF, Caramalho JC, Cabral Í. Influence of the mesenchymal stromal cell source on the hematopoietic supportive capacity of umbilical cord blood-derived CD34+-enriched cells. *Stem Cell Res Ther*. 2021;12:1–16. <https://doi.org/10.1186/S13287-021-02474-8/FIGURES/6>.
 84. Budgude P, Kale V, Vaidya A. Cryopreservation of mesenchymal stromal cell-derived extracellular vesicles using Trehalose maintains their ability to expand hematopoietic stem cells in vitro. *Cryobiology*. 2021;98:152–63. <https://doi.org/10.1016/J.CRYOBIOL.2020.11.009>.
 85. Blazquez R, Miguel Sanchez-Margallo F, de la Rosa O, Dalemans W, Álvarez V, Tarazona R, et al. Immunomodulatory potential of human adipose mesenchymal stem cells derived exosomes on in vitro stimulated T cells. *Front Immunol*. 2014;5. <https://doi.org/10.3389/fimmu.2014.00556>.
 86. Guo L, Lai P, Wang Y, Huang T, Chen X, Geng S, et al. Extracellular vesicles derived from mesenchymal stem cells prevent skin fibrosis in the cGVHD mouse model by suppressing the activation of macrophages and B cells immune response. *Int Immunopharmacol*. 2020;84:106541. <https://doi.org/10.1016/J.INTIMP.2020.106541>.
 87. Pinto DS, Ahsan T, Serra J, Fernandes-Platzgummer A, Cabral JMS, Silva CL. Modulation of the in vitro angiogenic potential of human mesenchymal stromal cells from different tissue sources. *J Cell Physiol*. 2020;235:7224–38. <https://doi.org/10.1002/jcp.29622>.
 88. Silva RM, Rosa SS, Santos JAL, Azevedo AM, Fernandes-Platzgummer A. Enabling mesenchymal stromal cells and their extracellular vesicles clinical Availability—A technological and economical evaluation. *J Extracell Biology*. 2025;4:e70037. <https://doi.org/10.1002/JEX2.70037>.

Publisher's note

Springer Nature remains neutral with regard to jurisdictional claims in published maps and institutional affiliations.